

# The entropy based goodness of fit tests for generalized von Mises–Fisher distributions and beyond

Nikolai Leonenko<sup>1</sup>, Vitalii Makogin \*<sup>2</sup>, and Mehmet Siddik Cadirci<sup>1</sup>

<sup>1</sup>School of Mathematics, Cardiff University,

Senghenydd Road, Cardiff, Wales, UK, CF24 4AG.

<sup>2</sup>Institute of Stochastics, Ulm University, Ulm, 08069 Germany.

October 22, 2020

## Abstract

We introduce some new classes of unimodal rotational invariant directional distributions, which generalize von Mises–Fisher distribution. We propose three types of distributions, one of which represents axial data. For each new type we provide formulae and short computational study of parameter estimators by the method of moments and the method of maximum likelihood. The main goal of the paper is to develop the goodness of fit test to detect that sample entries follow one of the introduced generalized von Mises–Fisher distribution based on the maximum entropy principle. We use  $k$ th nearest neighbour distances estimator of Shannon entropy and prove its  $L^2$ -consistency. We examine the behaviour of the test statistics, find critical values and compute power of the test on simulated samples. We apply the goodness of fit test to local fiber directions in a glass fibre reinforced composite material and detect the samples which follow axial generalized von Mises–Fisher distribution.

**Keywords**— Directional distribution, Generalized von Mises–Fisher distribution, Goodness of fit test, Entropy estimation, Maximum entropy principle, Nearest neighbour estimator.

## 1 Introduction

Directional distributions characterize randomness in unit vectors (directions). Spherical data sets appear in a wide range of problems arising from Earth sciences (Pischutta et al., 2013), oceanography (Wyatt et al., 1997; Shabani et al., 2016), biology (Mouritsen & Mouritsen, 2000), physics (Torrance et al., 1966), material science (Dresvyanskiy et al., 2020).

In this paper, we consider some classes of random unit vectors with values on sphere  $\mathbb{S}^{d-1} = \{\mathbf{x} \in \mathbb{R}^d : \|\mathbf{x}\| = 1\}$ , which have the absolutely continuous directional distributions with respect to the uniform distribution on  $\mathbb{S}^{d-1}$ . We denote by  $\mathbf{a}^\top \mathbf{b}$  the scalar product of vectors  $\mathbf{a}, \mathbf{b} \in \mathbb{R}^d$  and by  $\|\mathbf{a}\|$  the Euclidean norm of  $\mathbf{a} \in \mathbb{R}^d$ .

The von Mises–Fisher distribution is a fundamental isotropic distribution which is widely used in directional statistics (e.g. Mardia & Jupp, 2000, p. 168). It belongs to the exponential family of distributions, is rotational invariant and has a density proportional to  $\exp(\kappa \boldsymbol{\mu}^\top \mathbf{x})$ ,  $\mathbf{x} \in \mathbb{S}^{d-1}$ , such that random vectors are concentrated with rate  $\kappa \in \mathbb{R}$  along direction  $\boldsymbol{\mu} \in \mathbb{S}^{d-1}$ . Among several important properties of the von Mises–Fisher distribution we focus on maximum entropy characterization, that is, the von Mises–Fisher distribution has maximum entropy in the class of continuous distributions on  $\mathbb{S}^{d-1}$  with a given value of  $\mathbf{E}(X)$  (see Mardia, 1975).

There are several generalizations, including the Fisher–Bingham distribution with a density proportional to  $\exp(\kappa \boldsymbol{\mu}^\top \mathbf{x} + \mathbf{x}^\top A \mathbf{x})$ ,  $\mathbf{x} \in \mathbb{S}^{d-1}$  (see Mardia, 1975), and the generalized von Mises–Fisher

---

\*Corresponding author (e-mail: vitalii.makogin@uni-ulm.de). The research was partially supported by DFG Grant 390879134.

distribution of order  $k$  (GvMF $_k$ ) introduced in Gatto & Jammalamadaka (2007), having the density proportional to  $\exp\left(\sum_{j=1}^k \kappa_j (\boldsymbol{\mu}_j^\top \mathbf{x})^{r_j}\right)$ , where  $\boldsymbol{\mu}_j \in \mathbb{S}^{d-1}$ ,  $\kappa_j \in \mathbb{R}$ ,  $r_j \in \mathbb{N}$  ( $j = 1, \dots, k$ ), and  $r_1 \leq \dots \leq r_k$ .

In this paper, we introduce a new generalization of the von Mises–Fisher distribution, which stays in the exponential family and is rotational invariant with one mode. In contrast to the generalized von Mises–Fisher distribution of order  $k$  with integer power  $r \in \mathbb{N}$ , we consider densities with arbitrary positive power  $r \in \mathbb{R}_+$ . The motivation of such choice is to provide the analogue of a generalized Gaussian distribution for random vectors on the unit sphere. To do so we introduce the following three types of distributions of order  $\alpha \in \mathbb{R}_+$ , whose densities  $f$  are proportional to

$$\begin{aligned} \text{Type I, GvMF}_{1,d}(\alpha, \kappa, \boldsymbol{\mu}) : \quad f(\mathbf{x}) &\propto \exp\left(\frac{\kappa}{\alpha}(\boldsymbol{\mu}^\top \mathbf{x})^{<\alpha>}\right), \mathbf{x} \in \mathbb{S}^{d-1}, \\ \text{Type II, GvMF}_{2,d}(\alpha, \kappa, \boldsymbol{\mu}) : \quad f(\mathbf{x}) &\propto \exp\left(\frac{\kappa}{2\alpha} \|\mathbf{x} - \boldsymbol{\mu}\|^{2\alpha}\right), \mathbf{x} \in \mathbb{S}^{d-1}, \\ \text{Axial Type, GvMF}_{3,d}(\alpha, \kappa, \boldsymbol{\mu}) : \quad f(\mathbf{x}) &\propto \exp\left(\frac{\kappa}{\alpha} |\boldsymbol{\mu}^\top \mathbf{x}|^\alpha\right), \mathbf{x} \in \mathbb{S}^{d-1}, \end{aligned}$$

where  $\kappa > 0$  is a concentration parameter, and  $\boldsymbol{\mu} \in \mathbb{S}^{d-1}$  is a mean direction parameter. In the paper we denote by  $x^{<\alpha>} = |x|^\alpha \operatorname{sgn}(x)$ ,  $x \in \mathbb{R}$ .

Apart from studying the properties, simulations and parameter estimation for distributions GvMF $_{j,d}$  ( $j = 1, 2, 3$ ), we develop the goodness of fit test based on the estimation of the Shannon entropy and independent identically distributed (i.i.d.) sample. These tests exploit the maximum entropy principle, which is also proved in the paper as the spherical analogue of the results by Lutwak et al. (2004).

To do so, we employ the entropy estimators  $\hat{H}_{N,k}$  derived from  $k$ th nearest neighbour distances. Starting from the pioneering paper (Kozachenko & Leonenko, 1987), which proves by direct probability methods the consistency of  $\hat{H}_{N,1}$  for random vectors with values in Euclidean space, a large number of authors considered extending the class of admissible distributions and improved the convergence of  $\hat{H}_{N,k}$ , see Berrett et al. (2019); Bulinski & Dimitrov (2019); Delattre & Fournier (2017); Evans (2008); Evans et al. (2002); Gao et al. (2018); Goria et al. (2005); Leonenko et al. (2008), and the references therein. In (Li et al., 2011; Misra et al., 2010), the  $k$ th nearest neighbour entropy estimation is generalized for hyperspherical distributions.

Unlike the above mentioned works, the limit theory for point processes with a fixed  $k$  allows to prove the  $L^p$ -consistency of functionals of  $k$ th nearest neighbour distances for a wider class of distributions. The nearest neighbours method of estimation of the Shannon entropy for manifolds, including spheres, was developed by Penrose & Yukich (2013). In the present paper, we continue their work and prove the  $L^2$ -consistency of  $\hat{H}_{N,k}$ , as  $N \rightarrow \infty$  with arbitrary  $k \geq 1$  and for a random vector on a Riemannian manifold if its density is bounded and has compact support, see Theorem 4.6. Therefore, we show that  $\hat{H}_{N,k}$  is a consistent estimator for the samples from the introduced generalized von Mises–Fisher distributions.

From the recent papers, we mention (Berrett et al., 2019), where the efficient entropy estimation is provided via the weighted  $k$ th nearest neighbour distances with  $k = k_N$  depending on sample size  $N$ . Moreover, Berrett & Samworth (2019) introduced a non-parametric entropy based test of independence for multidimensional data. Lund & Jammalamadaka (2000) considered the entropy based test of goodness of fit for the von Mises distribution on the circle and used a different entropy estimate. Our study is motivated, particularly, by the work of Cadirci et al. (2020), where the entropy based goodness of fit test for generalized Gaussian distribution is given.

We verify our theoretical results by computational study on simulated samples and show the inflation of variances of  $\hat{H}_{N,k}$  as  $k$  grows, which confirms the conclusion of Berrett et al. (2019). Moreover, we detect the evidence of generalized von Mises–Fisher distributions in real world data by the presented entropy based goodness of fit test. Particularly, we find the evidence in 3D images of a glass fibre reinforced composite material, where fiber directions follow a generalized von Mises–Fisher distribution of axial type.

The manuscript is organized as follows. In Section 2, we revise the basic facts for von Mises–Fisher distribution. In Section 3, we introduce our three types of generalized von Mises–Fisher distribution and compute their moments (Section 3.1). Section 4 is devoted to the Shannon entropy of generalized von Mises–Fisher distributions and we show the maximum entropy principle for them in Section 4.1. Then we discuss the statistical estimation of an entropy and prove the  $L^2$  convergence of  $k$ th nearest neighbour estimator for random variables on compact manifolds (Section 4.2). In section 5, we formulate the maximum likelihood estimators (Section 5.1) and estimators by the method of moments for distributions GvMF $_{1,d}$ , GvMF $_{2,d}$ , and GvMF $_{3,d}$  (Section 5.2). In Section 6 we develop goodness of fit tests based on the maximum entropy principle for GvMF $_{2,d}$  (Section 6.1) and GvMF $_{1,d}$ , GvMF $_{3,d}$  (Section 6.2)

distributions. Results of numerical experiments on simulated samples are given in Section 7. We present the method of simulations in Section 7.1, parameter estimation in Section 7.2, entropy estimation in Section 3.7, and study of the test statistics in Section 7.4. In Section 8, we detect the generalized von Mises-Fisher distributions in a real data set. Some auxiliary material is given in the Appendix.

## 2 Preliminaries

In this section we provide some known facts needed for the sequel. Let  $\sigma(d\mathbf{x})$  be spherical measure on the sphere  $\mathbb{S}^{d-1}$ . It can be written in polar coordinates  $\mathbf{x} = (1, \mathbf{u}), 1 > 0, \mathbf{u} \in \mathbb{S}^{d-1}$  as

$$\sigma(d\mathbf{x}) = \frac{\Gamma(\frac{d}{2})}{2\pi^{d/2}} d\mathbf{u}.$$

**Lemma 2.1** ((Fang & Zhang, 1990, Lemma 2.5.1)). *Let  $g : \mathbb{R} \rightarrow \mathbb{R}_+$  be a non-negative Borel function,  $c > 0$  and  $\mathbf{a} = (a_1, \dots, a_m) \neq \mathbf{0}$ . Then*

$$\int_{\mathbf{x}^T \mathbf{x} = c^2} g(\mathbf{a}^T \mathbf{x}) \sigma(d\mathbf{x}) = \frac{2c\pi^{\frac{d-1}{2}}}{\Gamma(\frac{d-1}{2})} \int_{-c}^c g(\|\mathbf{a}\|y)(c^2 - y^2)^{\frac{d-3}{2}} dy. \quad (1)$$

In particular, if  $\mathbf{a} \in \mathbb{S}^{d-1}$ , then

$$\int_{\mathbf{x}^T \mathbf{x} = 1} g(\mathbf{a}^T \mathbf{x}) \sigma(d\mathbf{x}) = \frac{2\pi^{\frac{d-1}{2}}}{\Gamma(\frac{d-1}{2})} \int_{-1}^1 g(y)(1 - y^2)^{\frac{d-3}{2}} dy. \quad (2)$$

**Definition 2.1.** *A unit random vector  $\boldsymbol{\xi}$  has the  $(d-1)$ -dimensional von Mises-Fisher distribution  $\text{vMF}_{1,d}(\boldsymbol{\mu}, \kappa)$  if its probability density function with respect to the uniform distribution is*

$$f_{\boldsymbol{\xi}}(\mathbf{x}) = \left(\frac{\kappa}{2}\right)^2 \frac{1}{\Gamma(\frac{d}{2}) I_{\frac{d}{2}-1}(\kappa)} \exp(\kappa \boldsymbol{\mu}^T \mathbf{x}), \mathbf{x} \in \mathbb{S}^{d-1}, \quad (3)$$

where  $\kappa \in \mathbb{R}$ ,  $\boldsymbol{\mu} \in \mathbb{S}^{d-1}$  and  $I_\nu$  is the modified Bessel function of order  $\nu \geq 0$ .

In the case  $d = 3$  von Mises-Fisher distribution  $M_{1,3}(\boldsymbol{\mu}, \kappa)$  is called *Fisher distribution*. In this case formula (3) simplifies to  $f_{\boldsymbol{\xi}}(\mathbf{x}) = \frac{\kappa}{2 \sinh \kappa} \exp(\kappa \boldsymbol{\mu}^T \mathbf{x}), \mathbf{x} \in \mathbb{S}^2$ .

The density of  $M_{1,d}(\boldsymbol{\mu}, \kappa)$  can be written in the alternative form.

**Definition 2.2.** *A unit random vector  $\boldsymbol{\xi}$  has the  $(d-1)$ -dimensional von Mises-Fisher distribution  $\text{vMF}_{2,d}(\boldsymbol{\mu}, \kappa)$  if its probability density function with respect to the uniform distribution is*

$$f_{\boldsymbol{\xi}}(\mathbf{x}) = \left(\frac{\kappa}{2}\right)^2 \frac{e^\kappa}{\Gamma(\frac{d}{2}) I_{\frac{d}{2}-1}(\kappa)} \exp\left(-\frac{\kappa}{2} \|\mathbf{x} - \boldsymbol{\mu}\|^2\right), \mathbf{x} \in \mathbb{S}^{d-1}, \quad (4)$$

where  $\kappa \in \mathbb{R}$ ,  $\boldsymbol{\mu} \in \mathbb{S}^{d-1}$ .

Indeed,  $\frac{\kappa}{2} \|\mathbf{x} - \boldsymbol{\mu}\|^2 = \frac{\kappa}{2} \|\mathbf{x}\|^2 + \frac{\kappa}{2} \|\boldsymbol{\mu}\|^2 - \kappa \boldsymbol{\mu}^T \mathbf{x} = \kappa - \kappa \boldsymbol{\mu}^T \mathbf{x}$  for  $\mathbf{x}, \boldsymbol{\mu} \in \mathbb{S}^{d-1}$ . Particularly, the density of distribution  $M_{2,3}(\boldsymbol{\mu}, \kappa)$  equals  $\frac{\kappa}{1 - \exp(-2\kappa)} \exp\left(-\frac{\kappa}{2} \|\mathbf{x} - \boldsymbol{\mu}\|^2\right), \mathbf{x} \in \mathbb{S}^2$ .

Let us recall the standard directional statistics.

**Definition 2.3.** *Let  $\mathbf{X}$  be random vector with values in  $\mathbb{S}^{d-1}$  and  $\mathbf{E}\mathbf{X} \neq \mathbf{0}$ . A mean direction of  $\mathbf{X}$  is a vector  $\frac{\mathbf{E}\mathbf{X}}{\|\mathbf{E}\mathbf{X}\|}$ . A mean resultant length is  $\|\mathbf{E}\mathbf{X}\|$ .*

The mean resultant length is invariant and the mean direction is equivariant under rotation. Formally, let  $U \in SO(d)$  be a rotation matrix, then  $\|\mathbf{E}U\mathbf{X}\| = \|\mathbf{E}\mathbf{X}\|$  and  $\frac{\mathbf{E}U\mathbf{X}}{\|\mathbf{E}U\mathbf{X}\|} = U \frac{\mathbf{E}\mathbf{X}}{\|\mathbf{E}\mathbf{X}\|}$ .

Consider the class of distributions on  $\mathbb{S}^{d-1}$  with rotational symmetry, that is their distribution functions have a form  $f(\mathbf{x}) = g(\boldsymbol{\mu}^T \mathbf{x})$ ,  $\mathbf{x}, \boldsymbol{\mu} \in \mathbb{S}^{d-1}$ , e.g. (Bingham & Mardia, 1975). Such random vectors  $\mathbf{X}$  posses a *tangent-normal decomposition*

$$\mathbf{X} = (\boldsymbol{\mu}^T \mathbf{X}) \boldsymbol{\mu} + \sqrt{1 - (\boldsymbol{\mu}^T \mathbf{X})^2} \mathbf{Y}, \quad (5)$$

where  $\boldsymbol{\mu}^T \mathbf{X}$  and  $\mathbf{Y}$  are independent,  $\boldsymbol{\mu} \perp \mathbf{Y}$ , and  $\mathbf{Y}$  is uniformly distributed on  $\mathbb{S}^{d-2}$ . It follows from (5), that the mean resultant length is  $\|\mathbf{E}\mathbf{X}\| = \mathbf{E}[\boldsymbol{\mu}^T \mathbf{X}]$  and the mean direction equals  $\boldsymbol{\mu}$ .

### 3 Generalized von Mises-Fisher distributions

In this section we introduce our generalizations of the von Mises-Fisher distribution. We call  $\kappa \in \mathbb{R}$  a concentration parameter and  $\boldsymbol{\mu} \in \mathbb{S}^{d-1}$  a mean direction parameter.

**Definition 3.1.** A unit random vector  $\boldsymbol{\xi}$  has the  $(d-1)$ -dimensional I-type generalized von Mises-Fisher distribution  $\text{GvMF}_{1,d}(\alpha, \kappa, \boldsymbol{\mu})$  of order  $\alpha > 0$  if its probability density function with respect to the uniform distribution is

$$f_{\boldsymbol{\xi}}(\mathbf{x}) = c_{1,d}(\kappa, \alpha) \exp\left(\frac{\kappa}{\alpha}(\boldsymbol{\mu}^T \mathbf{x})^{<\alpha>}\right), \mathbf{x} \in \mathbb{S}^{d-1}, \quad (6)$$

where

$$c_{1,d}(\kappa, \alpha) = \left( \frac{2\pi^{\frac{d-1}{2}}}{\Gamma\left(\frac{d-1}{2}\right)} \int_0^1 \left(e^{\frac{\kappa}{\alpha}y^\alpha} + e^{-\frac{\kappa}{\alpha}y^\alpha}\right) (1-y^2)^{\frac{d-3}{2}} dy \right)^{-1}. \quad (7)$$

As an analogue of von Mises-Fisher distribution in the form  $\text{vMF}_{2,d}$ , we introduce the following class.

**Definition 3.2.** A unit random vector  $\boldsymbol{\xi}$  has the  $(d-1)$ -dimensional II-type generalized von Mises-Fisher distribution  $\text{GvMF}_{2,d}(\alpha, \kappa, \boldsymbol{\mu})$  of order  $\alpha > 0$  if its probability density function with respect to the uniform distribution is

$$f_{\boldsymbol{\xi}}(\mathbf{x}) = c_{2,d}(\kappa, \alpha) \exp\left(-\frac{\kappa}{2^\alpha \alpha} \|\mathbf{x} - \boldsymbol{\mu}\|^{2\alpha}\right), \mathbf{x} \in \mathbb{S}^{d-1}, \quad (8)$$

where

$$c_{2,d}(\kappa, \alpha) = \left( \frac{2\pi^{\frac{d-1}{2}}}{\Gamma\left(\frac{d-1}{2}\right)} \int_0^1 \left(e^{-\frac{\kappa}{\alpha}(1-y)^\alpha} + e^{-\frac{\kappa}{\alpha}(1+y)^\alpha}\right) (1-y^2)^{\frac{d-3}{2}} dy \right)^{-1}. \quad (9)$$

In the case of  $\alpha = 1$ , the introduced distributions  $\text{GvMF}_{1,d}$  and  $\text{GvMF}_{2,d}$  become the von Mises-Fisher distributions  $\text{vMF}_{1,d}$  and  $\text{vMF}_{2,d}$  respectively.

If we do not distinguish opposite directions we deal with axec. Commonly used technique in this case is to consider symmetric density functions  $f$  such that  $f(\mathbf{x}) = f(-\mathbf{x})$ ,  $\mathbf{x} \in \mathbb{S}^{d-1}$ . Since our motivation is to stay in the class of rotational invariant densities and to generalize the von Mises-Fisher distribution, we propose the following model for an axial data.

**Definition 3.3.** A unit random vector  $\boldsymbol{\xi}$  has the  $(d-1)$ -dimensional axial generalized von Mises-Fisher distribution  $\text{GvMF}_{3,d}(\alpha, \kappa, \boldsymbol{\mu})$  (or distribution of axial type) of order  $\alpha > 0$  if its probability density function with respect to the uniform distribution is

$$f_{\boldsymbol{\xi}}(\mathbf{x}) = c_{3,d}(\kappa, \alpha) \exp\left(\frac{\kappa}{\alpha} |\boldsymbol{\mu}^T \mathbf{x}|^\alpha\right), \mathbf{x} \in \mathbb{S}^{d-1}, \quad (10)$$

where  $\kappa \in \mathbb{R}$ ,  $\boldsymbol{\mu} \in \mathbb{S}^{d-1}$  and

$$c_{3,d}(\kappa, \alpha) = \left( \frac{4\pi^{\frac{d-1}{2}}}{\Gamma\left(\frac{d-1}{2}\right)} \int_0^1 e^{\frac{\kappa}{\alpha}y^\alpha} (1-y^2)^{\frac{d-3}{2}} dy \right)^{-1}. \quad (11)$$

*Remark 3.1.* Let us check that  $\int_{\mathbb{S}^{d-1}} f_{\boldsymbol{\xi}}(\mathbf{x}) \sigma(d\mathbf{x}) = 1$ . Then, the constant  $c_{1,d}(\kappa, \alpha)$  equals

$$\begin{aligned} & \left( \int_{\mathbb{S}^{d-1}} \exp\left(\frac{\kappa}{\alpha}(\boldsymbol{\mu}^T \mathbf{x})^{<\alpha>}\right) \sigma(d\mathbf{x}) \right)^{-1} \\ & \stackrel{(2)}{=} \left( \frac{2\pi^{\frac{d-1}{2}}}{\Gamma\left(\frac{d-1}{2}\right)} \int_{-1}^1 \exp\left(\frac{\kappa}{\alpha}y^{<\alpha>}\right) (1-y^2)^{\frac{d-3}{2}} dy \right)^{-1} \\ & = \left( \frac{2\pi^{\frac{d-1}{2}}}{\Gamma\left(\frac{d-1}{2}\right)} \int_0^1 \left(e^{\frac{\kappa}{\alpha}y^\alpha} + e^{-\frac{\kappa}{\alpha}y^\alpha}\right) (1-y^2)^{\frac{d-3}{2}} dy \right)^{-1}. \end{aligned}$$

Similarly, the constant  $c_{2,d}(\kappa, \alpha)$  equals

$$\begin{aligned} & \left( \int_{\mathbb{S}^{d-1}} \exp\left(-\frac{\kappa}{2^\alpha \alpha} \|\mathbf{x} - \boldsymbol{\mu}\|^{2\alpha}\right) \sigma(d\mathbf{x}) \right)^{-1} = \left( \int_{\mathbb{S}^{d-1}} \exp\left(-\frac{\kappa}{\alpha} (1 - \boldsymbol{\mu}^T \mathbf{x})^\alpha\right) \sigma(d\mathbf{x}) \right)^{-1} \\ & \stackrel{(2)}{=} \left( \frac{2\pi^{\frac{d-1}{2}}}{\Gamma\left(\frac{d-1}{2}\right)} \int_{-1}^1 \exp\left(-\frac{\kappa}{\alpha} (1-y)^\alpha\right) (1-y^2)^{\frac{d-3}{2}} dy \right)^{-1} \\ & = \left( \frac{2\pi^{\frac{d-1}{2}}}{\Gamma\left(\frac{d-1}{2}\right)} \int_0^1 \left(e^{-\frac{\kappa}{\alpha}(1-y)^\alpha} + e^{-\frac{\kappa}{\alpha}(1+y)^\alpha}\right) (1-y^2)^{\frac{d-3}{2}} dy \right)^{-1}. \end{aligned}$$

In the case  $\alpha = 2$ , the generalized von Mises-Fisher distribution of axial type reduces to the Watson distribution.

### 3.1 Moments

In this section we consider moments characteristics of  $\text{GvMF}_{j,d}(\alpha, \kappa, \boldsymbol{\mu})$ ,  $j = 1, 2, 3$  distributions. Denote by

$$A_{1,d}(\kappa, \alpha, \beta) = \int_0^1 e^{\frac{\kappa}{\alpha}y^\alpha} y^\beta (1-y^2)^{\frac{d-3}{2}} dy, \quad (12)$$

$$A_{2,d}(\kappa, \alpha, \beta) = \int_0^2 e^{-\frac{\kappa}{\alpha}y^\alpha} (2-y)^{\frac{d-3}{2}} y^{\frac{d-3}{2}+\beta} dy. \quad (13)$$

**Proposition 3.1.** Let  $\beta \geq 0$  and  $\mathbf{X} \sim \text{GvMF}_{1,d}(\alpha, \kappa, \boldsymbol{\mu})$ , then

$$\mathbf{E}((\boldsymbol{\mu}^T \mathbf{X})^{<\beta>}) = \frac{A_{1,d}(\kappa, \alpha, \beta) - A_{1,d}(-\kappa, \alpha, \beta)}{A_{1,d}(\kappa, \alpha, 0) + A_{1,d}(-\kappa, \alpha, 0)}. \quad (14)$$

*Proof.* Let  $f$  be the density of the form (6), then

$$\begin{aligned} \mathbf{E}((\boldsymbol{\mu}^T \mathbf{X})^{<\beta>}) &= \int_{\mathbb{S}^{d-1}} (\boldsymbol{\mu}^T \mathbf{x})^{<\beta>} f(\mathbf{x}) \sigma(d\mathbf{x}) \\ &\stackrel{(2)}{=} c_{1,d}(\kappa, \alpha) \frac{2\pi^{\frac{d-1}{2}}}{\Gamma(\frac{d-1}{2})} \int_{-1}^1 y^{<\beta>} \exp\left(\frac{\kappa}{\alpha}y^{<\alpha>}\right) (1-y^2)^{\frac{d-3}{2}} dy \\ &= c_{1,d}(\kappa, \alpha) \frac{2\pi^{\frac{d-1}{2}}}{\Gamma(\frac{d-1}{2})} \int_0^1 \left(e^{\frac{\kappa}{\alpha}y^\alpha} - e^{-\frac{\kappa}{\alpha}y^\alpha}\right) y^\beta (1-y^2)^{\frac{d-3}{2}} dy \\ &= \frac{\int_0^1 (e^{\frac{\kappa}{\alpha}y^\alpha} - e^{-\frac{\kappa}{\alpha}y^\alpha}) y^\beta (1-y^2)^{\frac{d-3}{2}} dy}{\int_0^1 (e^{\frac{\kappa}{\alpha}y^\alpha} + e^{-\frac{\kappa}{\alpha}y^\alpha}) (1-y^2)^{\frac{d-3}{2}} dy}. \end{aligned}$$

□

Particularly, the mean direction of  $\mathbf{X} \sim \text{GvMF}_{1,d}(\alpha, \kappa, \boldsymbol{\mu})$  is  $\boldsymbol{\mu}$  and its mean resultant length equals

$$\|\mathbf{E}[\mathbf{X}]\| = \mathbf{E}[\boldsymbol{\mu}^T \mathbf{X}] = \frac{A_{1,d}(\kappa, \alpha, 1) - A_{1,d}(-\kappa, \alpha, 1)}{A_{1,d}(\kappa, \alpha, 0) + A_{1,d}(-\kappa, \alpha, 0)}. \quad (15)$$

**Proposition 3.2.** Let  $\beta \geq 0$  and  $\mathbf{X} \sim \text{GvMF}_{2,d}(\alpha, \kappa, \boldsymbol{\mu})$ , then

$$\mathbf{E}\|\mathbf{X} - \boldsymbol{\mu}\|^{2\beta} = 2^\beta \frac{A_{2,d}(\kappa, \alpha, \beta)}{A_{2,d}(\kappa, \alpha, 0)}. \quad (16)$$

*Proof.* Let  $f$  be the density of the form (8), then

$$\begin{aligned} \mathbf{E}\|\mathbf{X} - \boldsymbol{\mu}\|^{2\beta} &= \int_{\mathbb{S}^{d-1}} \|\mathbf{x} - \boldsymbol{\mu}\|^{2\beta} f(\mathbf{x}) \sigma(d\mathbf{x}) = \int_{\mathbb{S}^{d-1}} (2 - 2\boldsymbol{\mu}^T \mathbf{x})^\beta f(\mathbf{x}) \sigma(d\mathbf{x}) \\ &\stackrel{(2)}{=} c_{2,d}(\kappa, \alpha) \frac{2\pi^{\frac{d-1}{2}}}{\Gamma(\frac{d-1}{2})} \int_{-1}^1 (2 - 2y)^\beta \exp\left(-\frac{\kappa}{\alpha}(1-y)^\alpha\right) (1-y^2)^{\frac{d-3}{2}} dy \\ &= 2^\beta \frac{\int_{-1}^1 (1-y)^\beta e^{-\frac{\kappa}{\alpha}(1-y)^\alpha} (1-y^2)^{\frac{d-3}{2}} dy}{\int_{-1}^1 e^{-\frac{\kappa}{\alpha}(1-y)^\alpha} (1-y^2)^{\frac{d-3}{2}} dy} \\ &= 2^\beta \frac{\int_0^2 e^{-\frac{\kappa}{\alpha}z^\alpha} (2-z)^{\frac{d-3}{2}} z^{\frac{d-3}{2}+\beta} dz}{\int_0^2 e^{-\frac{\kappa}{\alpha}z^\alpha} (2-z)^{\frac{d-3}{2}} z^{\frac{d-3}{2}} dz}. \end{aligned}$$

□

Particularly, the mean direction of  $\mathbf{X} \sim \text{GvMF}_{2,d}(\alpha, \kappa, \boldsymbol{\mu})$  is  $\boldsymbol{\mu}$  and its mean resultant length equals

$$\|\mathbf{E}[\mathbf{X}]\| = \mathbf{E}[\boldsymbol{\mu}^T \mathbf{X}] = 1 - \frac{A_{2,d}(\kappa, \alpha, 1)}{A_{2,d}(\kappa, \alpha, 0)}. \quad (17)$$

**Proposition 3.3.** Let  $\beta \geq 0$  and  $\mathbf{X} \sim \text{GvMF}_{3,d}(\alpha, \kappa, \boldsymbol{\mu})$ , then

$$\mathbf{E}(|\boldsymbol{\mu}^T \mathbf{X}|^\beta) = \frac{A_{1,d}(\kappa, \alpha, \beta)}{A_{1,d}(\kappa, \alpha, 0)}. \quad (18)$$

*Proof.* Let  $f$  be the density of the form (10), then

$$\begin{aligned} \mathbf{E}(|\boldsymbol{\mu}^T \mathbf{X}|^\beta) &= \int_{\mathbb{S}^{d-1}} |\boldsymbol{\mu}^T \mathbf{x}|^\beta f(\mathbf{x}) \sigma(d\mathbf{x}) \\ &\stackrel{(2)}{=} c_{3,d}(\kappa, \alpha) \frac{2\pi^{\frac{d-1}{2}}}{\Gamma(\frac{d-1}{2})} \int_{-1}^1 |y|^\beta \exp\left(\frac{\kappa}{\alpha}|y|^\alpha\right) (1-y^2)^{\frac{d-3}{2}} dy \\ &= \frac{\int_0^1 e^{\frac{\kappa}{\alpha}y^\alpha} y^\beta (1-y^2)^{\frac{d-3}{2}} dy}{\int_0^1 e^{\frac{\kappa}{\alpha}y^\alpha} (1-y^2)^{\frac{d-3}{2}} dy}. \end{aligned}$$

□

Note that, the mean direction of  $\mathbf{X} \sim \text{GvMF}_{3,d}(\alpha, \kappa, \boldsymbol{\mu})$  is not defined and its mean resultant length  $\|\mathbf{E}[\mathbf{X}]\| = \mathbf{E}[\boldsymbol{\mu}^T \mathbf{X}]$  equals 0.

## 4 Entropy

In this section we find the entropy of generalized von Mises–Fisher distributions, and show the maximum entropy principle for them. Then we discuss the statistical estimation of an entropy and prove the  $L^2$  convergence of the  $k$ th nearest neighbour estimator for random variables on compact manifolds.

### 4.1 Maximum entropy principle for generalized von-Mises Fisher distributions

Recall that the entropy of a continuous random vector  $\mathbf{X} \in \mathbb{S}^{d-1}$  with a density  $f$  is

$$H(\mathbf{X}) = - \int_{\mathbb{S}^{d-1}} (\log f(\mathbf{x})) f(\mathbf{x}) \sigma(d\mathbf{x}). \quad (19)$$

For a density version  $f$  we denote its support by  $\text{supp } f = \{\mathbf{x} \in \mathbb{S}^{d-1} : f(\mathbf{x}) > 0\}$ . Clearly, the integral in (19) is taken over  $\text{supp } f$ .

**Theorem 4.1.** Let  $\mathbf{X}_j \sim \text{GvMF}_{j,d}(\alpha, \kappa, \boldsymbol{\mu})$ ,  $j = 1, 2, 3$ , then

$$H(\mathbf{X}_1) = -\log c_{1,d}(\kappa, \alpha) - \frac{\kappa}{\alpha} \mathbf{E}((\boldsymbol{\mu}^T \mathbf{X}_1)^{<\alpha>}), \quad (20)$$

$$H(\mathbf{X}_2) = -\log c_{2,d}(\kappa, \alpha) + \frac{\kappa}{2^\alpha \alpha} \mathbf{E}\|\mathbf{X}_2 - \boldsymbol{\mu}\|^{2\alpha} \quad (21)$$

$$H(\mathbf{X}_3) = -\log c_{3,d}(\kappa, \alpha) - \frac{\kappa}{\alpha} \mathbf{E}|\boldsymbol{\mu}^T \mathbf{X}_3|^\alpha. \quad (22)$$

*Proof.* Let  $\mathbf{X}_1$  have density  $f_1$ , then the entropy of  $\mathbf{X}_1$  equals

$$\begin{aligned} - \int_{\mathbb{S}^{d-1}} (\log f_1(\mathbf{x})) f_1(\mathbf{x}) \sigma(d\mathbf{x}) &= -\log c_{1,d}(\kappa, \alpha) \int_{\mathbb{S}^{d-1}} f_1(\mathbf{x}) \sigma(d\mathbf{x}) \\ - \frac{\kappa}{\alpha} \int_{\mathbb{S}^{d-1}} (\boldsymbol{\mu}^T \mathbf{x})^{<\alpha>} f_1(\mathbf{x}) \sigma(d\mathbf{x}) &= -\log c_{1,d}(\kappa, \alpha) - \frac{\kappa}{\alpha} \mathbf{E}((\boldsymbol{\mu}^T \mathbf{X}_1)^{<\alpha>}). \end{aligned}$$

For  $\mathbf{X}_2$  with density  $f_2$  we have

$$\begin{aligned} H(\mathbf{X}_2) &= - \int_{\mathbb{S}^{d-1}} (\log f_2(\mathbf{x})) f_2(\mathbf{x}) \sigma(d\mathbf{x}) = -\log c_{2,d}(\kappa, \alpha) \int_{\mathbb{S}^{d-1}} f_2(\mathbf{x}) \sigma(d\mathbf{x}) \\ &+ \frac{\kappa}{2^\alpha \alpha} \int_{\mathbb{S}^{d-1}} \|\mathbf{x} - \boldsymbol{\mu}\|^{2\alpha} f_2(\mathbf{x}) \sigma(d\mathbf{x}) = -\log c_{2,d}(\kappa, \alpha) + \frac{\kappa}{2^\alpha \alpha} \mathbf{E}\|\mathbf{X}_2 - \boldsymbol{\mu}\|^{2\alpha}. \end{aligned}$$

The case of  $\mathbf{X}_3$  is similar. □

**Theorem 4.2.** Let a unit random vector  $\mathbf{Z} \in \mathbb{S}^{d-1}$  have a generalized von Mises-Fisher distribution  $\text{GvMF}_{1,d}(\alpha, \kappa, \boldsymbol{\mu})$ . Then  $\mathbf{Z}$  has the maximum entropy value over all continuous random variables  $\mathbf{X}$  on  $\mathbb{S}^{d-1}$  with

$$\mathbf{E}((\boldsymbol{\mu}^T \mathbf{X})^{<\alpha>}) = \mathbf{E}((\boldsymbol{\mu}^T \mathbf{Z})^{<\alpha>}). \quad (23)$$

*Proof.* Let  $\mathbf{X}$  be a random unit vector on  $\mathbb{S}^{d-1}, d \geq 2$  such that (23) holds true. Let  $f$  and  $f^*$  be the densities of  $\mathbf{X}$  and  $\mathbf{Z}$  respectively. By Jensen's inequality,

$$\begin{aligned} & \int_{\mathbb{S}^{d-1}} f(\mathbf{x}) \log f^*(\mathbf{x}) \sigma(d\mathbf{x}) - \int_{\mathbb{S}^{d-1}} f(\mathbf{x}) \log f(\mathbf{x}) \sigma(d\mathbf{x}) = \int_{\mathbb{S}^{d-1}} f(\mathbf{x}) \log \frac{f^*(\mathbf{x})}{f(\mathbf{x})} \sigma(d\mathbf{x}) \\ & \leq \log \left( \int_{\mathbb{S}^{d-1}} f(\mathbf{x}) \frac{f^*(\mathbf{x})}{f(\mathbf{x})} \sigma(d\mathbf{x}) \right) = 0 \end{aligned}$$

with equality if and only if  $f = f^*$  almost everywhere with respect to the Lebesgue measure on  $\mathbb{S}^{d-1}$ . So,

$$H(\mathbf{X}) = - \int_{\mathbb{S}^{d-1}} f(\mathbf{x}) \log f(\mathbf{x}) \sigma(d\mathbf{x}) \leq - \int_{\mathbb{S}^{d-1}} f(\mathbf{x}) \log f^*(\mathbf{x}) \sigma(d\mathbf{x}). \quad (24)$$

In this case  $f^*(\mathbf{x}) = \log c_{1,d}(\kappa, \alpha) + \frac{\kappa}{\alpha} (\boldsymbol{\mu}^T \mathbf{x})^{<\alpha>}, \mathbf{x} \in \mathbb{S}^{d-1}$  and hence

$$\begin{aligned} H(\mathbf{X}) & \leq - \int_{\mathbb{S}^{d-1}} f(\mathbf{x}) \log f^*(\mathbf{x}) \sigma(d\mathbf{x}) = - \log c_{1,d}(\kappa, \alpha) - \frac{\kappa}{\alpha} \int_{\mathbb{S}^{d-1}} (\boldsymbol{\mu}^T \mathbf{x})^{<\alpha>} f(\mathbf{x}) \sigma(d\mathbf{x}) \\ & = - \log c_{1,d}(\kappa, \alpha) - \frac{\kappa}{\alpha} \mathbf{E}[(\boldsymbol{\mu}^T \mathbf{X})^{<\alpha>}] = - \log c_{1,d}(\kappa, \alpha) - \frac{\kappa}{\alpha} \mathbf{E}[(\boldsymbol{\mu}^T \mathbf{Z})^{<\alpha>}] \\ & = - \log c_{1,d}(\kappa, \alpha) - \frac{\kappa}{\alpha} \int_{\mathbb{S}^{d-1}} (\boldsymbol{\mu}^T \mathbf{x})^{<\alpha>} f^*(\mathbf{x}) \sigma(d\mathbf{x}) \\ & = - \int_{\mathbb{S}^{d-1}} f^*(\mathbf{x}) \log f^*(\mathbf{x}) \sigma(d\mathbf{x}) = H(\mathbf{Z}). \end{aligned}$$

□

The maximum entropy principle for generalized von Mises-Fisher distribution of type II has the following form.

**Theorem 4.3.** Let a unit random vector  $\mathbf{Z} \in \mathbb{S}^{d-1}$  have a generalized von Mises-Fisher distribution  $\text{GvMF}_{2,d}(\alpha, \kappa, \boldsymbol{\mu})$ . Then  $\mathbf{Z}$  has the maximum entropy value over all continuous random variables  $\mathbf{X}$  on  $\mathbb{S}^{d-1}$  with

$$\mathbf{E}\|\mathbf{X} - \boldsymbol{\mu}\|^{2\alpha} = \mathbf{E}\|\mathbf{Z} - \boldsymbol{\mu}\|^{2\alpha}. \quad (25)$$

*Proof.* Let  $f$  and  $f^*$  be the densities of  $\mathbf{X}$  and  $\mathbf{Z}$  respectively. The proof is similar to Theorem 4.2. Indeed,  $f^*(\mathbf{x}) = \log c_{2,d}(\kappa, \alpha) - \frac{\kappa}{2^\alpha \alpha} \|\mathbf{x} - \boldsymbol{\mu}\|^{2\alpha}, \mathbf{x} \in \mathbb{S}^{d-1}$  and hence

$$\begin{aligned} H(\mathbf{X}) & \leq - \int_{\mathbb{S}^{d-1}} f(\mathbf{x}) \log f^*(\mathbf{x}) \sigma(d\mathbf{x}) = - \log c_{2,d}(\kappa, \alpha) + \frac{\kappa}{2^\alpha \alpha} \int_{\mathbb{S}^{d-1}} \|\mathbf{x} - \boldsymbol{\mu}\|^{2\alpha} f(\mathbf{x}) \sigma(d\mathbf{x}) \\ & = - \log c_{2,d}(\kappa, \alpha) + \frac{\kappa}{2^\alpha \alpha} \mathbf{E}\|\mathbf{X} - \boldsymbol{\mu}\|^{2\alpha} = - \log c_{2,d}(\kappa, \alpha) + \frac{\kappa}{2^\alpha \alpha} \mathbf{E}\|\mathbf{Z} - \boldsymbol{\mu}\|^{2\alpha} \\ & = - \log c_{2,d}(\kappa, \alpha) + \frac{\kappa}{2^\alpha \alpha} \int_{\mathbb{S}^{d-1}} \|\mathbf{x} - \boldsymbol{\mu}\|^{2\alpha} f^*(\mathbf{x}) \sigma(d\mathbf{x}) = - \int_{\mathbb{S}^{d-1}} f^*(\mathbf{x}) \log f^*(\mathbf{x}) \sigma(d\mathbf{x}) = H(\mathbf{Z}). \end{aligned}$$

□

**Theorem 4.4.** Let a unit random vector  $\mathbf{Z} \in \mathbb{S}^{d-1}$  have an axial generalized von Mises-Fisher distribution  $\text{GvMF}_{3,d}(\alpha, \kappa, \boldsymbol{\mu})$ . Then  $\mathbf{Z}$  has the maximum entropy value over all continuous random variables  $\mathbf{X}$  on  $\mathbb{S}^{d-1}$  with

$$\mathbf{E}|\boldsymbol{\mu}^T \mathbf{X}|^\alpha = \mathbf{E}|\boldsymbol{\mu}^T \mathbf{Z}|^\alpha. \quad (26)$$

*Proof.* The proof is similar to Theorems 4.2 and 4.3. In this case,  $f^*(\mathbf{x}) = \log c_{3,d}(\kappa, \alpha) + \frac{\kappa}{\alpha} |\boldsymbol{\mu}^T \mathbf{x}|^\alpha, \mathbf{x} \in \mathbb{S}^{d-1}$  and

$$\begin{aligned} H(\mathbf{X}) & \leq - \log c_{3,d}(\kappa, \alpha) - \frac{\kappa}{\alpha} \int_{\mathbb{S}^{d-1}} |\boldsymbol{\mu}^T \mathbf{x}|^\alpha f(\mathbf{x}) \sigma(d\mathbf{x}) \\ & = - \log c_{3,d}(\kappa, \alpha) - \frac{\kappa}{\alpha} \mathbf{E}|\boldsymbol{\mu}^T \mathbf{X}|^\alpha = - \log c_{3,d}(\kappa, \alpha) - \frac{\kappa}{\alpha} \mathbf{E}|\boldsymbol{\mu}^T \mathbf{Z}|^\alpha = H(\mathbf{Z}). \end{aligned}$$

□

## 4.2 Entropy estimation

In this section we give the method of an entropy estimation for unit random vectors. Actually, we extend the phase-state to the arbitrary compact Riemannian manifold.

Let  $m, d \in \mathbb{N}$ ,  $m \leq d$ , and  $\mathcal{M}$  be a  $m$ -dimensional  $C^1$  manifold embedded in  $\mathbb{R}^d$  with the atlas  $((U_i, g_i), i \in I_0)$ , i.e., for each  $y \in \mathcal{M}$  there exists an open subset  $U_i$  of  $\mathbb{R}^m$  and a continuously differentiable injection  $g_i : U_i \rightarrow \mathbb{R}^d$ , such that  $y \in g_i(U) \subset \mathcal{M}$ , and  $g_i$  is an open map from  $U_i$  to  $\mathcal{M}$ , and the linear map  $g'_i(u)$  has full rank for all  $u \in U_i$ .

For bounded measurable  $h : \mathcal{M} \rightarrow \mathbb{R}$ , the integral  $\int_{\mathcal{M}} h(y)\nu(dy)$  is defined by

$$\int_{\mathcal{M}} h(y)\nu(dy) = \sum_{i \in I_0} \int_{U_i} h(g_i(x))\psi_i(g_i(x))\sqrt{\det(J_{g_i}(x))'(J_{g_i}(x))}dx,$$

where  $\nu$  is a  $\sigma$ -finite measure on  $\mathcal{M}$ ,  $J_{g_i}$  is the Jacobian of  $g_i$  and  $\{\psi_i, i \in I_0\}$  is the partition of unity, see (Penrose & Yukich, 2013, pp. 3–4) and (Berger & Gostiaux, 1988, Chapter 2) for more detailed setting.

Let  $f : \mathcal{M} \rightarrow \mathbb{R}_+$  be a probability density of independent random elements  $X, X_i, i \in \mathbb{N}$  with values in  $\mathcal{M}$ , i.e.,  $\int_{\mathcal{M}} f(x)\nu(dx) = 1$ . Denote by  $\mathcal{X}_N = \{X_1, \dots, X_N\}$ ,  $N \geq k$  the samples of the first  $N$  elements. The entropy of  $X$  equals  $H(X) = -\int_{\mathcal{M}} \log(f(x))f(x)\nu(dx)$ . Let  $F$  be a finite subset of  $\{X_i, i \geq k\}$  and  $\rho_k(x, F)$  be the Euclidean distance between  $x$  and its  $k$ th nearest neighbour in  $F \setminus \{x\}$ . Let  $\gamma \approx 0.5772$  be the Euler–Mascheroni constant.

**Definition 4.1.** *The  $k$ –nearest neighbour estimator ( $k$ –NNE) of the entropy  $H(X)$  is defined by*

$$\widehat{H}_{N,k}(\mathcal{X}_N) = \frac{1}{N} \sum_{i=1}^N \log \left( \rho_k^m(X_i, \mathcal{X}_N) V_m(N-1) e^{-\psi(k)} \right), \quad (27)$$

where

$$\psi(k) = \sum_{j=1}^{k-1} \frac{1}{j} - \gamma, \quad V_m = \frac{\pi^{m/2}}{\Gamma(1+m/2)}.$$

For example, if  $k = 1$ , then the nearest neighbour distances estimator (NNE) is

$$\widehat{H}_{N,1}(\mathcal{X}_N) = \frac{m}{N} \sum_{i=1}^N \log \rho_{N,1,i} + \log V_m + \gamma + \log(N-1). \quad (28)$$

We start the proof of  $L^2$ -consistency of  $\widehat{H}_{N,k}$  by writing down the particular case of Theorem 3.1 from (Penrose & Yukich, 2013) for the functional

$$\xi(x, \mathcal{X}) := \log \left( e^{-\psi(k)} V_m \rho_k^m(x, \mathcal{X}) \right). \quad (29)$$

**Theorem 4.5.** *Let  $k \geq 1$  put  $q = 1$  or  $q = 2$ . Suppose there exists  $p \geq q$  such that*

$$\sup_{N \geq k} \mathbf{E} \left| \xi \left( N^{\frac{1}{m}} X_1, N^{\frac{1}{m}} \mathcal{X}_N \right) \right|^p < \infty. \quad (30)$$

Then as  $N \rightarrow \infty$  we have  $L^q$  convergence

$$\frac{1}{N} \sum_{x \in \mathcal{X}_N} \xi \left( N^{\frac{1}{m}} x, N^{\frac{1}{m}} \mathcal{X}_N \right) \rightarrow \int_{\mathcal{M}} \mathbf{E}[\xi(\mathbf{0}, \mathcal{P}_{f(x)})] f(x) \nu(dx), \quad (31)$$

where  $\mathcal{P}_{\lambda}$  denotes a homogeneous Poisson point process of intensity  $\lambda > 0$  in  $\mathbb{R}^m$  (embedded in  $\mathbb{R}^d$ ).

For the bounded random variables  $X_i, i \geq 1$  and  $\rho_k(x, \mathcal{X}_N)$ , we generalize Lemma 7.8 from (Penrose & Yukich, 2013), which was proved for the case  $k = 1$ .

**Lemma 4.1.** *Let  $f$  is bounded and has compact support on  $\mathcal{M}$ , then for any  $\delta \in (0, m)$*

$$\sup_{N \geq k} \mathbf{E} \left[ \rho_k^{\delta} \left( N^{\frac{1}{m}} X_1, N^{\frac{1}{m}} \mathcal{X}_N \right) \right] < \infty.$$

*Proof.* The proof is very similar to (Penrose & Yukich, 2013, Lemma 7.8). Recall that  $\mathcal{M}$  has the atlas  $((U_i, g_i), i \in I_0)$ , where  $I_0 = \{1, \dots, i_0\}$ , and there exist  $\delta_i, x_i, i \in I_0$  such that  $\mathcal{M} \in \cup_{i \in I_0} B_{\delta_i}(y_i)$ .

Denote  $A_i = B_{\delta_i} \setminus \cup_{j < i} B_{\delta_j}(y_j)$ . Since  $\text{supp}(f)$  is bounded then there exist  $i_0 \in \mathbb{N}$  and constant  $C > 0$  such that

$$\begin{aligned} \mathbf{E} \left[ N^{\frac{\delta}{m}} \rho_k^\delta(X_1, \mathcal{X}_N) \right] &= N^{\frac{\delta}{m}-1} \mathbf{E} \left( \sum_{x \in \mathcal{X}_N} \rho_k^\delta(x, \mathcal{X}_N) \right) \\ &\leq N^{\frac{\delta}{m}-1} \left[ \sum_{i=1}^{i_0} \sum_{x \in A_i \cap \mathcal{X}_N} \rho_k^\delta(x, A_i \cap \mathcal{X}_N) + C \right]. \end{aligned} \quad (32)$$

Now we prove that for all finite  $\mathcal{Y} \subset A_i$

$$\sum_{x \in \mathcal{Y}} \rho_k^\delta(x, \mathcal{Y}) \leq C_i [\text{card}(\mathcal{Y})]^{1-\frac{\delta}{m}}.$$

where  $C_i > 0$ . Let  $\mathcal{Y} \subset A_i$  and  $y_j \in \mathcal{Y}$  be a the  $j$ th nearest neighbour of  $x \in \mathcal{Y}$ . Taking  $z_j \in \mathcal{Y}$  such that  $g_i^{-1}(z_j)$  to be  $j$ -th nearest neighbour of  $g_i^{-1}(x)$  in  $g_i^{-1}(\mathcal{Y})$ , we have from (Penrose & Yukich, 2013, Lemma 4.1) that

$$\begin{aligned} \rho_k(x, \mathcal{Y}) &= \max\{\|y_1 - x\|, \dots, \|y_k - x\|\} \leq \max\{\|z_1 - x\|, \dots, \|z_k - x\|\} \\ &\leq C_i \max\{\|g_i^{-1}(z_1) - g_i^{-1}(x)\|, \dots, \|g_i^{-1}(z_k) - g_i^{-1}(x)\|\} = C_i \rho_k(g_i^{-1}(x), g_i^{-1}(\mathcal{Y})). \end{aligned}$$

Thus, from (Yukich, 2006, Lemma 3.3) we have for any  $\delta \in (0, m)$

$$\sum_{x \in A_i \cap \mathcal{X}_N} \rho_k^\delta(x, A_i \cap \mathcal{X}_N) \leq C_i [\text{diam}(g_i^{-1}(A_i \cap \mathcal{X}_N))]^\delta [\text{card}(g_i^{-1}(A_i \cap \mathcal{X}_N))]^{1-\frac{\delta}{m}} \leq \tilde{C}_i N^{1-\frac{\delta}{m}}.$$

Hence, the right hand side of (32) is bounded above uniformly.  $\square$

Now we prove the  $L^2$ -convergence of the  $k$ th nearest neighbour estimator

$$\hat{H}_{N,k}(\mathcal{X}_N) = \frac{1}{N} \sum_{x \in \mathcal{X}_N} \xi \left( N^{\frac{1}{m}} x, N^{\frac{1}{m}} \mathcal{X}_N \right), \quad (33)$$

which is an extension from the case  $k = 1$  to  $k \geq 1$  of Theorem 2.4. from (Penrose & Yukich, 2013).

**Theorem 4.6.** Suppose  $f$  is bounded and has compact support. Then for every fixed  $k \geq 1$

$$\mathbf{E} \left[ \hat{H}_{N,k}(\mathcal{X}_N) - H(X) \right]^2 \rightarrow 0 \quad \text{as } N \rightarrow \infty. \quad (34)$$

*Proof.* We apply Theorem 4.5. Repeating the lines of the proof of (Cadirci et al., 2020, Theorem 3), we compute  $\mathbf{E}[\xi(\mathbf{0}, \mathcal{P}_\lambda)]$ , where

$$\xi(\mathbf{0}, \mathcal{P}_\lambda) = \log V_m - \psi(k) + m \log \rho_k(\mathbf{0}, \mathcal{P}_\lambda).$$

The random variable  $\rho_k(\mathbf{0}, \mathcal{P}_\lambda)$  is the distance to the  $k$ th point of  $\mathcal{P}_\lambda$  from  $\mathbf{0}$ . Therefore,

$$\begin{aligned} \mathbb{P}(\rho_k(\mathbf{0}, \mathcal{P}_\lambda) \leq t) &= \mathbb{P}(\mathcal{P}_\lambda \cap B_t(\mathbf{0}) \geq k) \\ &= 1 - \sum_{j=0}^{k-1} \frac{1}{j!} e^{-\lambda |B_t(\mathbf{0})|} (\lambda |B_t(\mathbf{0})|)^j = 1 - \sum_{j=0}^{k-1} \frac{1}{j!} e^{-\lambda t^m V_m} (\lambda t^m V_m)^j, t \geq 0. \end{aligned}$$

Then

$$\begin{aligned} m \mathbf{E}[\log \rho_k(\mathbf{0}, \mathcal{P}_\lambda)] &= \int_0^\infty \log t^m \frac{(\lambda V_m)^k (t^m)^{(k-1)}}{(k-1)!} e^{-\lambda V_m t^m} m t^{m-1} dt \\ &= -\log(\lambda V_m) + \int_0^\infty \log y \frac{y^{k-1}}{(k-1)!} e^{-y} dy \\ &= -\log \lambda - \log V_m + \psi(k). \end{aligned}$$

Thus,

$$\int_{\mathcal{M}} \mathbf{E}[\xi(\mathbf{0}, \mathcal{P}_{f(x)})] f(x) \nu(dx) = - \int_{\mathcal{M}} (\log f(x)) f(x) \nu(dx) = H(X).$$

Second, we check condition (30). Note that for every  $\delta \in (0, 1)$  and  $p > 1$  there exists  $C > 0$  such that  $|\log t|^p \leq Ct^{-\delta} \mathbb{1}_{[0,1]}(t) + Ct^{\delta} \mathbb{1}_{[1,\infty)}(t)$ ,  $t > 0$ . Then

$$\begin{aligned} \mathbf{E} \left| \xi \left( N^{\frac{1}{m}} X_1, N^{\frac{1}{m}} \mathcal{X}_N \right) \right|^p &\leq 2^{p-1} |\log V_m - \psi(k)|^p + 2^{p-1} \mathbf{E} \left| \log \rho_k^m \left( N^{\frac{1}{m}} X_1, N^{\frac{1}{m}} \mathcal{X}_N \right) \right|^p \\ &\leq 2^{p-1} |\log V_m - \psi(k)|^p \\ &+ 2^{p-1} C \mathbf{E} \rho_k^{-\delta} \left( N^{\frac{1}{m}} X_1, N^{\frac{1}{m}} \mathcal{X}_N \right) \mathbb{1}_{[0,1]} \left( \rho_k^\delta \left( N^{\frac{1}{m}} X_1, N^{\frac{1}{m}} \mathcal{X}_N \right) \right) \quad (35) \end{aligned}$$

$$+ 2^{p-1} C \mathbf{E} \rho_k^\delta \left( N^{\frac{1}{m}} X_1, N^{\frac{1}{m}} \mathcal{X}_N \right) \mathbb{1}_{[1,\infty)} \left( \rho_k^\delta \left( N^{\frac{1}{m}} X_1, N^{\frac{1}{m}} \mathcal{X}_N \right) \right). \quad (36)$$

Term (35) is finite because

$$\begin{aligned} &\sup_{N \geq k} \mathbf{E} \rho_k^{-\delta} \left( N^{\frac{1}{m}} X_1, N^{\frac{1}{m}} \mathcal{X}_N \right) \mathbb{1}_{[0,1]} \left( \rho_k^\delta \left( N^{\frac{1}{m}} X_1, N^{\frac{1}{m}} \mathcal{X}_N \right) \right) \\ &\leq \sup_{N \geq k} \mathbf{E} \rho_1^{-\delta} \left( N^{\frac{1}{m}} X_1, N^{\frac{1}{m}} \mathcal{X}_N \right) < \infty, \end{aligned} \quad (37)$$

where (37) is ensured by (Penrose & Yukich, 2013, Lemma 7.5) if  $f$  is bounded and  $\delta \in (0, m)$ . Hence, for (30) to be satisfied, it remains to show that

$$\sup_{N \geq k} \mathbf{E} \rho_k^\delta \left( N^{\frac{1}{m}} X_1, N^{\frac{1}{m}} \mathcal{X}_N \right) < \infty. \quad (38)$$

Thus, applying Lemma 4.1 we get that (38) holds true if  $0 < \delta < m$ .  $\square$

The 2-dimensional sphere  $\mathbb{S}^2$  is a compact manifold with  $d = 3$ ,  $m = 2$  and  $\nu = \sigma$ . Thus, Theorem 4.3 is valid for all bounded densities on  $\mathbb{S}^2$ ,  $k$ th nearest neighbour estimator has the form

$$\widehat{H}_{N,k}(\mathcal{X}_N) = \frac{2}{N} \sum_{i=1}^N \log \rho_k(X_i, \mathcal{X}_N) - \psi(k) + \log(N-1) + \log \pi,$$

and  $\widehat{H}_{N,k}(\mathcal{X}_N) \rightarrow H(X)$  in  $L^2(\Omega)$ . This yields, that  $\widehat{H}_{N,k}(\mathcal{X}_N)$  is a consistent estimator of the Shannon entropy.

## 5 Estimation of parameters

### 5.1 Fisher's maximum likelihood estimation

Let  $\mathcal{X}_N = \{\mathbf{x}_1, \dots, \mathbf{x}_N\}$  be a random sample. We write down the log-likelihood  $l(\mathcal{X}_N)$  for random samples from the introduced generalized von Mises-Fisher distributions.

**Lemma 5.1.** *Let  $\mathcal{X}_{j,N} \sim \text{GvMF}_{j,d}(\alpha, \kappa, \boldsymbol{\mu})$ ,  $j = 1, 2, 3$  then*

$$l(\mathcal{X}_{1,N}) = N \log c_{1,d}(\kappa, \alpha) + \frac{\kappa}{\alpha} \sum_{i=1}^N (\boldsymbol{\mu}^T \mathbf{x}_i)^{<\alpha>} \quad (39)$$

$$l(\mathcal{X}_{2,N}) = N \log c_{2,d}(\kappa, \alpha) - \frac{\kappa}{2^\alpha \alpha} \sum_{i=1}^N \|\mathbf{x}_i - \boldsymbol{\mu}\|^{2\alpha}, \quad (40)$$

$$l(\mathcal{X}_{3,N}) = N \log c_{3,d}(\kappa, \alpha) + \frac{\kappa}{\alpha} \sum_{i=1}^N |\boldsymbol{\mu}^T \mathbf{x}_i|^\alpha. \quad (41)$$

*Proof.* The statements follow from the direct calculation of  $l(\mathcal{X}_N)$ .  $\square$

In each case, we use numerical methods to find the maximum likelihood estimates  $(\hat{\mu}_L, \hat{\kappa}_L, \hat{\alpha}_L)$  of  $(\mu, \kappa, \alpha)$  which maximize the log-likelihoods (39)-(41).

The problem becomes easier when parameter  $\alpha$  is known. In such a case, we can derive maximum likelihood estimates taking derivatives of (39)-(41). In such a case, we have the estimates of  $\mu$  as  $\kappa$  as

- Let  $\mathcal{X}_N \sim \text{GvMF}_{1,d}(\alpha, \kappa, \boldsymbol{\mu})$ , then

$$\hat{\boldsymbol{\mu}}_L = \arg \max_{\boldsymbol{\mu} \in \mathbb{S}^{d-1}} \sum_{i=1}^N (\boldsymbol{\mu}^\top \mathbf{x}_i)^{<\alpha>}, \quad \frac{A_{1,d}(\hat{\kappa}_L, \alpha, \alpha) - A_{1,d}(-\hat{\kappa}_L, \alpha, \alpha)}{A_{1,d}(\hat{\kappa}_L, \alpha, 0) + A_{1,d}(-\hat{\kappa}_L, \alpha, 0)} = \frac{1}{N} \sum_{i=1}^N (\boldsymbol{\mu}_L^\top \mathbf{x}_i)^{<\alpha>}.$$

- Let  $\mathcal{X}_N \sim \text{GvMF}_{2,d}(\alpha, \kappa, \boldsymbol{\mu})$ , then

$$\hat{\boldsymbol{\mu}}_L = \arg \min_{\boldsymbol{\mu} \in \mathbb{S}^{d-1}} \sum_{i=1}^N \|\mathbf{x}_i - \boldsymbol{\mu}\|^{2\alpha}, \quad 2^\alpha \frac{A_{2,d}(\hat{\kappa}_L, \alpha, \alpha)}{A_{2,d}(\hat{\kappa}_L, \alpha, 0)} = \frac{1}{N} \sum_{i=1}^N \|\mathbf{x}_i - \hat{\boldsymbol{\mu}}_L\|^{2\alpha}. \quad (42)$$

- Let  $\mathcal{X}_N \sim \text{GvMF}_{3,d}(\alpha, \kappa, \boldsymbol{\mu})$ , then

$$\hat{\boldsymbol{\mu}}_L = \arg \max_{\boldsymbol{\mu} \in \mathbb{S}^{d-1}} \sum_{i=1}^N |\boldsymbol{\mu}^\top \mathbf{x}_i|^\alpha, \quad \frac{A_{1,d}(\hat{\kappa}_L, \alpha, \alpha)}{A_{1,d}(\hat{\kappa}_L, \alpha, 0)} = \frac{1}{N} \sum_{i=1}^N |\hat{\boldsymbol{\mu}}_L^\top \mathbf{x}_i|^\alpha. \quad (43)$$

## 5.2 Method of moments

In this section we consider parameter estimation of generalized von Mises-Fisher distributions based on moments estimation.

In the case of non-axial random vector  $\mathbf{X} \in \mathbb{S}^{d-1}$  we assume that  $\|\mathbf{E}\mathbf{X}\| \neq 0$ . We know from Definition 2.3 that  $\hat{\boldsymbol{\mu}} := \frac{\bar{\mathcal{X}}_N}{\|\bar{\mathcal{X}}_N\|}$ , where  $\bar{\mathcal{X}}_N = \frac{1}{N} \sum_{i=1}^N \mathbf{x}_i$ , is the natural estimator for mean direction parameter  $\boldsymbol{\mu}$ . In order to find estimates for parameters  $\alpha$  and  $\kappa$  we need at least two more moment statistics. A standard approach involves the use of the resultant length. For the second relations we choose  $\mathbf{E}(\text{sgn}\{\mathbf{X}_1^\top \mathbf{E}\mathbf{X}_1\})$  and  $\mathbf{E}(\|\mathbf{X}_2 - \boldsymbol{\mu}\|^4)$  for vectors  $\mathbf{X}_j \sim \text{GvMF}_{j,d}(\alpha, \kappa, \mu)$  ( $j = 1, 2$ ). Applying (15) and (17), one can get the estimators  $\hat{\kappa}, \hat{\alpha}$  as a solution of the following equations

$$\begin{aligned} \frac{A_{1,d}(\hat{\kappa}, \hat{\alpha}, 1) - A_{1,d}(-\hat{\kappa}, \hat{\alpha}, 1)}{A_{1,d}(\hat{\kappa}, \hat{\alpha}, 0) + A_{1,d}(-\hat{\kappa}, \hat{\alpha}, 0)} &= \|\bar{\mathcal{X}}_{1,N}\|, \quad \frac{A_{1,d}(\hat{\kappa}, \hat{\alpha}, 0) - A_{1,d}(-\hat{\kappa}, \hat{\alpha}, 0)}{A_{1,d}(\hat{\kappa}, \hat{\alpha}, 0) + A_{1,d}(-\hat{\kappa}, \hat{\alpha}, 0)} = \frac{\sum_{i=1}^N \text{sgn}(x_i^\top \bar{\mathcal{X}}_{1,N})}{N \|\bar{\mathcal{X}}_{1,N}\|}; \\ \frac{A_{2,d}(\hat{\kappa}, \hat{\alpha}, 1)}{A_{2,d}(\hat{\kappa}, \hat{\alpha}, 0)} &= 1 - \|\bar{\mathcal{X}}_{2,N}\|, \quad \frac{A_{2,d}(\hat{\kappa}, \hat{\alpha}, 2)}{A_{2,d}(\hat{\kappa}, \hat{\alpha}, 0)} = \frac{1}{4N} \sum_{i=1}^N \left\| x_i - \frac{\bar{\mathcal{X}}_{2,N}}{\|\bar{\mathcal{X}}_{2,N}\|} \right\|^4 \end{aligned}$$

for the samples  $\mathcal{X}_{1,N} \sim \text{GvMF}_{1,d}(\alpha, \kappa, \boldsymbol{\mu})$  and  $\mathcal{X}_{2,N} \sim \text{GvMF}_{2,d}(\alpha, \kappa, \boldsymbol{\mu})$ , respectively.

*Remark 5.1.* If the parameter  $\alpha$  is known, we can reduce the problem of the moment estimation to the solution of one equation. Namely,

$$\frac{A_{1,d}(\hat{\kappa}, \alpha, 1) - A_{1,d}(-\hat{\kappa}, \alpha, 1)}{A_{1,d}(\hat{\kappa}, \alpha, 0) + A_{1,d}(-\hat{\kappa}, \alpha, 0)} = \|\bar{\mathcal{X}}_{1,N}\|, \quad \text{and} \quad \frac{A_{2}(\hat{\kappa}, \alpha, 1)}{A_{2}(\hat{\kappa}, \alpha, 0)} = 1 - \|\bar{\mathcal{X}}_{2,N}\|.$$

In the case of a symmetrically distributed random vector  $\mathbf{X} \in \mathbb{S}^{d-1}$ ,  $\mathbf{E}\mathbf{X} = 0$  and the value  $\mathbf{E}\mathbf{X}/\|\mathbf{E}\mathbf{X}\|$  is not defined. Recall the tangent-normal decomposition (5) of a random vector  $\mathbf{X} \in \mathbb{S}^{d-1}$ , that is  $\mathbf{X} = \boldsymbol{\mu}\xi + \sqrt{1-\xi^2}\mathbf{Y}$ , where  $\boldsymbol{\mu} \in \mathbb{S}^{d-1}$  is a mean direction parameter,  $\xi$  is a random variable on  $[-1, 1]$  independent of a uniformly distributed random vector  $\mathbf{Y} \in \mathbb{S}^{d-2}$  such that  $\boldsymbol{\mu} \perp \mathbf{Y}$ .

To find relations which determine the parameter  $\boldsymbol{\mu}$  and distribution  $\xi$  we consider an orientation tensor  $T(\mathbf{X})$  given by

$$T(\mathbf{X}) = \mathbf{X}\mathbf{X}^\top = \xi^2 \boldsymbol{\mu}\boldsymbol{\mu}^\top + \xi\sqrt{1-\xi^2}(\boldsymbol{\mu}\mathbf{Y}^\top + \mathbf{Y}\boldsymbol{\mu}^\top) + (1-\xi^2)\mathbf{Y}\mathbf{Y}^\top. \quad (44)$$

Therefore, the mean orientation tensor is

$$\mathbf{E}T(\mathbf{X}) = \mathbf{E}[\mathbf{X}\mathbf{X}^\top] = \boldsymbol{\mu}\boldsymbol{\mu}^\top \mathbf{E}\xi^2 + (1 - \mathbf{E}\xi^2)\mathbf{E}\mathbf{Y}\mathbf{Y}^\top. \quad (45)$$

**Theorem 5.1.** *Let a random vector  $\mathbf{X}$  has a representation as above, i.e.,  $\mathbf{X} = \boldsymbol{\mu}\xi + \sqrt{1-\xi^2}\mathbf{Y}$ . Then*

$$\boldsymbol{\mu}\boldsymbol{\mu}^\top = \sqrt{\frac{d-1}{d\mathbf{E}[\mathbf{X}(\mathbf{E}\mathbf{X}\mathbf{X}^\top)\mathbf{X}^\top] - 1}} \left( \mathbf{E}\mathbf{X}\mathbf{X}^\top - \frac{1}{d}I_d \right) + \frac{1}{d}I_d, \quad (46)$$

$$\mathbf{E}\xi^2 = \frac{1}{d} + \sqrt{\frac{d-1}{d}} \sqrt{\mathbf{E}[\mathbf{X}(\mathbf{E}\mathbf{X}\mathbf{X}^\top)\mathbf{X}^\top] - \frac{1}{d}}, \quad (47)$$

$$\mathbf{E}\xi^4 = \mathbf{E} \left[ \mathbf{X}^\top \mathbf{E}T(\mathbf{X}) \mathbf{X} - \frac{1 - \mathbf{E}\xi^2}{d-1} \right]^2 \frac{d-1}{d\mathbf{E}[\mathbf{X}(\mathbf{E}\mathbf{X}\mathbf{X}^\top)\mathbf{X}^\top] - 1}. \quad (48)$$

where  $I_d$  is  $d \times d$  identity matrix.

*Proof.* Let  $U_{\boldsymbol{\mu}} \in SO(d)$ , such that  $\boldsymbol{\mu} = U_{\boldsymbol{\mu}} \mathbf{e}_x$ , where  $\mathbf{e}_x = (1, 0, \dots, 0)^T$ . Denote by  $\tilde{\mathbf{Y}} = U_{\boldsymbol{\mu}}^{-1} \mathbf{Y}$ . The vector  $\tilde{\mathbf{Y}}$  is uniformly distributed on  $\mathbb{S}^{d-2}$  with the first coordinate equal 0. Then  $\mathbf{X} = U_{\boldsymbol{\mu}} (\xi \mathbf{e}_x + \sqrt{1 - \xi^2} \tilde{\mathbf{Y}})$  and  $\mathbf{E} \mathbf{X} \mathbf{X}^T = U_{\boldsymbol{\mu}} \left( \mathbf{e}_x \mathbf{e}_x^T \mathbf{E} \xi^2 + (1 - \mathbf{E} \xi^2) \mathbf{E} \tilde{\mathbf{Y}} \tilde{\mathbf{Y}}^T \right) U_{\boldsymbol{\mu}}^{-1}$ . It follows from the symmetry that  $\mathbf{E} \tilde{\mathbf{Y}} \tilde{\mathbf{Y}}^T = \frac{1}{d-1} \begin{pmatrix} 0 & 0 \\ 0 & I_{d-1} \end{pmatrix}$ . Therefore,

$$\mathbf{E} \mathbf{X} \mathbf{X}^T = U_{\boldsymbol{\mu}} \left( \mathbf{e}_x \mathbf{e}_x^T \mathbf{E} \xi^2 + \frac{1 - \mathbf{E} \xi^2}{d-1} (I_d - \mathbf{e}_x \mathbf{e}_x^T) \right) U_{\boldsymbol{\mu}}^T = \mathbf{E} \xi^2 \boldsymbol{\mu} \boldsymbol{\mu}^T + \frac{1 - \mathbf{E} \xi^2}{d-1} (I_d - \boldsymbol{\mu} \boldsymbol{\mu}^T). \quad (49)$$

Thus,  $\boldsymbol{\mu} \boldsymbol{\mu}^T = \frac{d-1}{d \mathbf{E} \xi^2 - 1} \left( \mathbf{E} \mathbf{X} \mathbf{X}^T - \frac{1 - \mathbf{E} \xi^2}{d-1} \right)$ . Then consider  $\mathbf{X}^T \mathbf{E} T(\mathbf{X}) \mathbf{X}$ . From (49) we have

$$\mathbf{X}^T \mathbf{E} T(\mathbf{X}) \mathbf{X} = \mathbf{X}^T \boldsymbol{\mu} \boldsymbol{\mu}^T \mathbf{X} \mathbf{E} \xi^2 + \frac{1 - \mathbf{E} \xi^2}{d-1} (1 - \mathbf{X}^T \boldsymbol{\mu} \boldsymbol{\mu}^T \mathbf{X}) = \xi^2 \mathbf{E} \xi^2 + \frac{1 - \mathbf{E} \xi^2}{d-1} (1 - \xi^2).$$

and  $\mathbf{E} [\mathbf{X}^T \mathbf{E} T(\mathbf{X}) \mathbf{X}] = (\mathbf{E} \xi^2)^2 + \frac{(1 - \mathbf{E} \xi^2)^2}{d-1}$ . This yields  $\mathbf{E} \xi^2 = \frac{1}{d} + \sqrt{\frac{d-1}{d}} \sqrt{\mathbf{E} [\mathbf{X} (\mathbf{E} \mathbf{X} \mathbf{X}^T) \mathbf{X}^T] - \frac{1}{d}}$  and

$$\boldsymbol{\mu} \boldsymbol{\mu}^T = \sqrt{\frac{d-1}{d \mathbf{E} [\mathbf{X} (\mathbf{E} \mathbf{X} \mathbf{X}^T) \mathbf{X}^T] - 1}} \left( \mathbf{E} \mathbf{X} \mathbf{X}^T - \frac{1}{d} I_d \right) + \frac{1}{d} I_d.$$

Finally,

$$\mathbf{E} \left[ \mathbf{X}^T \mathbf{E} T(\mathbf{X}) \mathbf{X} - \frac{1 - \mathbf{E} \xi^2}{d-1} \right]^2 = \left( \frac{d \mathbf{E} \xi^2 - 1}{d-1} \right)^2 \mathbf{E} \xi^4.$$

□

Note, that for an axial vector  $\mathbf{X}$ , the random variable  $\xi$  has a symmetric distribution on  $[-1, 1]$ , therefore  $\mathbf{E} \xi = 0$ . So, if  $\xi$  has two-dimensional parametric distribution, one get from Theorem 5.1 the parameter estimates for  $\xi$ .

We apply Theorem 5.1 for the random sample  $\mathcal{X}_N = \{\mathbf{x}_1, \dots, \mathbf{x}_N\}$  from  $\text{GvMF}_{3,d}(\alpha, \kappa, \boldsymbol{\mu})$ . Denote by  $\bar{T} = \frac{1}{n} \sum_{i=1}^n \mathbf{x}_i \mathbf{x}_i'$ . Then  $\mathbf{E} \xi^2 = \mathbf{E}(\boldsymbol{\mu}' \mathbf{x}_1)^2$  and  $\mathbf{E} \xi^4 = \mathbf{E}(\boldsymbol{\mu}' \mathbf{x}_1)^4$  are given in Proposition 3.3.

**Corollary 5.1.1.** *Let  $\mathcal{X}_N \sim \text{GvMF}_{3,d}(\alpha, \kappa, \boldsymbol{\mu})$  and denote by  $\bar{T} = \frac{1}{N} \sum_{i=1}^N \mathbf{x}_i \mathbf{x}_i^T$  and  $\bar{V} = \frac{1}{N} \sum_{i=1}^N \mathbf{x}_i \bar{T} \mathbf{x}_i^T$ . Then (46)–(48) hold true and*

$$\begin{aligned} \hat{\boldsymbol{\mu}} \hat{\boldsymbol{\mu}}^T &= \sqrt{\frac{d-1}{d \bar{V} - 1}} \left( \bar{T} - \frac{1}{d} I_d \right) + \frac{1}{d} I_d, \quad \frac{A_1(\hat{\kappa}, \hat{\alpha}, 2)}{A_1(\kappa, \alpha, 0)} = \frac{1}{d} + \sqrt{\frac{d-1}{d}} \sqrt{\bar{V} - \frac{1}{d}}, \\ \frac{A_1(\kappa, \alpha, 4)}{A_1(\kappa, \alpha, 0)} &= \frac{d-1}{(d \bar{V} - 1) N} \sum_{i=1}^N \left( \mathbf{x}_i^T \bar{T} \mathbf{x}_i - \frac{1}{d} - \frac{\sqrt{d \bar{V} - 1}}{d \sqrt{d-1}} \right)^2. \end{aligned} \quad (50)$$

## 6 Goodness of fit test based on the maximum entropy principle

In this section we provide the statistical test for verification that a random sample follows a generalized von Mises-Fisher distribution. The methodology for all three introduced distributions is very similar. For simplicity, we provide detailed explanation for the Type-II distribution.

### 6.1 Type II

Denote by  $\text{GvMF}_{2,d}$  the class of generalized von Mises-Fisher distributions  $\text{GvMF}_{2,d}(\alpha, \kappa, \boldsymbol{\mu})$ ,  $\alpha > 0$ ,  $\kappa > 0$  and  $\boldsymbol{\mu} \in \mathbb{S}^{d-1}$ . Let  $\mathcal{X}_N = \{\mathbf{x}_1, \dots, \mathbf{x}_N\}$  be a random sample of vectors on a sphere  $\mathbb{S}^{d-1}$  and  $\mathbf{x}_j \stackrel{d}{=} \mathbf{X}, j = 1, \dots, N$  with unknown distribution.

Let  $\mathbf{Z} \sim \text{GvMF}_{2,d}(\alpha, \kappa, \boldsymbol{\mu})$ . From (13), (16), and Theorem 4.3 we know that  $H(\mathbf{Z}) \geq H(\mathbf{X})$  for all continuous random vectors  $\mathbf{X} \in \mathbb{S}^{d-1}$  with  $\mathbf{E} \|\mathbf{X} - \boldsymbol{\mu}\|^{2\alpha} = \mathbf{E} \|\mathbf{Z} - \boldsymbol{\mu}\|^{2\alpha} = 2^\alpha \frac{A_{2,d}(\kappa, \alpha, \alpha)}{A_{2,d}(\kappa, \alpha, 0)}$ . Using Theorem 4.1, we get

$$\inf_{\substack{\alpha, \kappa > 0, \\ \boldsymbol{\mu} \in \mathbb{S}^{d-1}}} \left\{ -\log c_{2,d}(\kappa, \alpha) + \frac{\kappa}{\alpha} \frac{A_{2,d}(\kappa, \alpha, \alpha)}{A_{2,d}(\kappa, \alpha, 0)} \middle| \mathbf{E} \|\mathbf{X} - \boldsymbol{\mu}\|^{2\alpha} = 2^\alpha \frac{A_{2,d}(\kappa, \alpha, \alpha)}{A_{2,d}(\kappa, \alpha, 0)} \right\} \geq H(\mathbf{X}). \quad (51)$$

Moreover, equality in (51) appears if and only if  $\mathbf{X}$  belongs to some distribution from the family  $\text{GvMF}_{2,d}$ . We substitute now the unobservable value of  $\mathbf{E}\|\mathbf{X} - \boldsymbol{\mu}\|^{2\alpha}$  by its statistical counterpart  $\frac{1}{N} \sum_{i=1}^N \|\mathbf{x}_i - \boldsymbol{\mu}\|^{2\alpha}$  and define the statistics

$$S_2(\mathcal{X}_N) = \inf_{\substack{\alpha, \kappa > 0, \\ \boldsymbol{\mu} \in \mathbb{S}^{d-1}}} \left\{ -\log c_{2,d}(\kappa, \alpha) + \frac{\kappa}{\alpha} \frac{A_{2,d}(\kappa, \alpha, \alpha)}{A_{2,d}(\kappa, \alpha, 0)} \middle| \frac{\sum_{i=1}^N \|\mathbf{x}_i - \boldsymbol{\mu}\|^{2\alpha}}{N^{2\alpha}} = \frac{A_{2,d}(\kappa, \alpha, \alpha)}{A_{2,d}(\kappa, \alpha, 0)} \right\}.$$

Consider the value under inf in  $S_2(\mathcal{X}_N)$ . Under the condition  $\frac{1}{N^{2\alpha}} \sum_{i=1}^N \|\mathbf{x}_i - \boldsymbol{\mu}\|^{2\alpha} = \frac{A_{2,d}(\kappa, \alpha, \alpha)}{A_{2,d}(\kappa, \alpha, 0)}$ , we have

$$-\log c_{2,d}(\kappa, \alpha) + \frac{\kappa}{\alpha} \frac{A_{2,d}(\kappa, \alpha, \alpha)}{A_{2,d}(\kappa, \alpha, 0)} = -\left( \log c_{2,d}(\kappa, \alpha) - \frac{\kappa}{\alpha 2^\alpha} \frac{1}{N} \sum_{i=1}^N \|\mathbf{x}_i - \boldsymbol{\mu}\|^{2\alpha} \right) = -\frac{l_2(\mathcal{X}_N)}{N}.$$

Thus,

$$S_2(\mathcal{X}_N) = -\frac{1}{N} \sup_{\substack{\alpha, \kappa > 0, \\ \boldsymbol{\mu} \in \mathbb{S}^{d-1}}} \left\{ l(\mathcal{X}_N) \middle| \frac{\sum_{i=1}^N \|\mathbf{x}_i - \boldsymbol{\mu}\|^{2\alpha}}{N^{2\alpha}} = \frac{A_{2,d}(\kappa, \alpha, \alpha)}{A_{2,d}(\kappa, \alpha, 0)} \right\}.$$

Let us consider unconditional maximization of log-likelihood  $l_2(\mathcal{X}_N)$ . Partial derivative with respect to  $\kappa$  equals

$$\begin{aligned} \frac{\partial l_2(\mathcal{X}_N)}{\partial \kappa} &= \frac{\partial}{\partial \kappa} \left( \log \frac{\Gamma(\frac{d-1}{2})}{2\pi^{\frac{d-1}{2}}} - \log A_{2,d}(\kappa, \alpha, 0) - \frac{\kappa}{\alpha 2^\alpha} \frac{1}{N} \sum_{i=1}^N \|\mathbf{x}_i - \boldsymbol{\mu}\|^{2\alpha} \right) \\ &= \frac{1}{\alpha} \frac{A_{2,d}(\kappa, \alpha, \alpha)}{A_{2,d}(\kappa, \alpha, 0)} - \frac{1}{\alpha 2^\alpha N} \sum_{i=1}^N \|\mathbf{x}_i - \boldsymbol{\mu}\|^{2\alpha}, \end{aligned}$$

where we used  $\frac{\partial}{\partial \kappa} A_{2,d}(\kappa, \alpha, 0) = -\frac{1}{\alpha} A_{2,d}(\kappa, \alpha, \alpha)$ . Thus, the superimum in  $S_2(\mathcal{X}_N)$  with respect to  $\kappa$  coincides with the unconditional supremum of  $l_2(\mathcal{X}_N)$  and

$$S_2(\mathcal{X}_N) = -\frac{1}{N} \sup_{\substack{\alpha, \kappa > 0, \\ \boldsymbol{\mu} \in \mathbb{S}^{d-1}}} l_2(\mathcal{X}_N). \quad (52)$$

Let  $\Theta_0$  be a compact subset of  $\mathbb{R}_+^2$  large enough to contain all values of parameters  $(\alpha, \kappa)$  appearing in practice. Consider the following hypotheses

- $H_{2,0} : X \sim \text{GvMF}_{2,d}$ , for some  $(\alpha, \kappa) \in \Theta_0$ ,
- $H_{2,1} : X \not\sim \text{GvMF}_{2,d}$  for all  $(\alpha, \kappa) \in \Theta_0$ .

Since  $\Theta_0$  is compact, maximum likelihood estimators  $\hat{\alpha}_L, \hat{\kappa}_L$  are consistent. We proved in Theorem (4.6) that the  $k$ th nearest neighbour estimator  $\hat{H}_{N,k}$  of  $H(\mathbf{X})$  is  $L^2$ -consistent for any  $k \in \mathbb{N}$ . Thus, we test  $H_{2,0}$  vs.  $H_{2,1}$  with the statistic

$$\hat{T}_{2,k}^L(\mathcal{X}_N) := -\log c_{2,d}(\hat{\kappa}_L, \hat{\alpha}_L) + \frac{\hat{\kappa}_L}{\hat{\alpha}_L} \frac{A_{2,d}(\hat{\kappa}_L, \hat{\alpha}_L, \hat{\alpha}_L)}{A_{2,d}(\hat{\kappa}_L, \hat{\alpha}_L, 0)} - \hat{H}_{N,k} \quad (53)$$

which tends in probability to 0, as  $N \rightarrow \infty$ . We reject  $H_{2,0}$  with level of significance  $\beta$  if  $|\hat{T}_{2,k}^L(\mathcal{X}_N)| \geq x_\beta$ , where  $x_\beta$  is a critical value determined by  $\mathbb{P}_{H_0}(|\hat{T}_{2,k}^L(\mathcal{X}_N)| \geq x_\beta) \leq \beta$ .

*Remark 6.1.* It is easy to see that maximum likelihood estimates of  $\alpha, \kappa$ , estimator  $\hat{H}_{N,k}$  and the statistics  $\hat{T}_{2,k}^L$  are rotational invariant.

Actually, we can replace the maximum likelihood estimates of  $\alpha, \kappa$  in (53) by any consistent estimates  $\hat{\alpha}, \hat{\kappa}$ . Indeed, if  $\mathbf{x}_1 \sim \text{GvMF}_{2,d}(\alpha, \kappa, \boldsymbol{\mu})$  under hypothesis  $H_0$ , then

$$2^{\hat{\alpha}} \frac{A_{2,d}(\hat{\kappa}, \hat{\alpha}, \hat{\alpha})}{A_{2,d}(\hat{\kappa}, \hat{\alpha}, 0)} \xrightarrow[N \rightarrow \infty]{P} 2^\alpha \frac{A_{2,d}(\kappa, \alpha, \alpha)}{A_{2,d}(\kappa, \alpha, 0)} = \mathbf{E}\|\mathbf{x}_1 - \boldsymbol{\mu}\|^\alpha$$

and

$$\hat{T}_{2,k}(\mathcal{X}_N) := -\log c_{2,d}(\hat{\kappa}, \hat{\alpha}) + \frac{\hat{\kappa}}{\hat{\alpha}} \frac{A_{2,d}(\hat{\kappa}, \hat{\alpha}, \hat{\alpha})}{A_{2,d}(\hat{\kappa}, \hat{\alpha}, 0)} - \hat{H}_{N,k} \xrightarrow[\text{under } H_0]{P} H(\mathbf{x}_1) - H(\mathbf{x}_1) = 0$$

as  $N \rightarrow \infty$ .

The critical values  $x_\beta$  can be found by Monte Carlo simulations of test statistics  $\hat{T}_{2,N}^L$  or  $\hat{T}_{2,N}$ .

## 6.2 Type I and axial data

The goodness of fit test for the axial generalized von-Mises distribution and the distribution of the I-type are constructed similarly to II-type distributions. Let  $\Theta_0$  be a compact subset of  $\mathbb{R}_+^2$  large enough to contain all values parameters  $(\alpha, \kappa)$  appearing in practice. Let  $j = 1, 3$  and consider the following hypotheses

- $H_{j,0} : X \sim \text{GvMF}_{j,d}$ , for some  $(\alpha, \kappa) \in \Theta_0$ ,
- $H_{j,1} : X \not\sim \text{GvMF}_{j,d}$  for all  $(\alpha, \kappa) \in \Theta_0$ .

For testing  $H_{1,0}$  vs.  $H_{1,1}$  we use the statistic  $\hat{T}_{1,N}$  given by

$$\hat{T}_{1,k}(\mathcal{X}_N) := -\log c_{1,d}(\hat{\kappa}, \hat{\alpha}) - \frac{\hat{\kappa}}{\hat{\alpha}} \frac{A_{1,d}(\hat{\kappa}, \hat{\alpha}, \hat{\alpha}) - A_{1,d}(-\hat{\kappa}, \hat{\alpha}, \hat{\alpha})}{A_{1,d}(\hat{\kappa}, \hat{\alpha}, 0) + A_{1,d}(-\hat{\kappa}, \hat{\alpha}, 0)} - \hat{H}_{N,k}, \quad (54)$$

where  $\hat{\alpha}, \hat{\kappa}$  are some consistent estimates of  $\alpha, \kappa$ .

For the axial distribution, we test  $H_{3,0}$  vs.  $H_{3,1}$  by the test statistic  $\hat{T}_{3,N}$  given by

$$\hat{T}_{3,k}(\mathcal{X}_N) := -\log c_{3,d}(\hat{\kappa}, \hat{\alpha}) - \frac{\hat{\kappa}}{\hat{\alpha}} \frac{A_{1,d}(\hat{\kappa}, \hat{\alpha}, \hat{\alpha})}{A_{1,d}(\hat{\kappa}, \hat{\alpha}, 0)} - \hat{H}_{N,k}, \quad (55)$$

where  $\hat{\alpha}, \hat{\kappa}$  are some consistent estimates of  $\alpha, \kappa$ .

## 7 Numerical experiments

### 7.1 Simulation

In this section, we provide the method for simulation of  $\text{GvMF}_{j,d}$  distributed random vectors and study the behaviour of the test statistic  $\hat{T}_{j,k}$  on simulated samples  $j = 1, 2, 3$ .

Let  $X_j \sim \text{GvMF}_{j,d}(\alpha, \kappa, \boldsymbol{\mu}), j = 1, 2, 3$ . Due to the tangent-normal decomposition

$$\mathbf{X}_j = (\boldsymbol{\mu}^\top \mathbf{X}_j) \boldsymbol{\mu} + \sqrt{1 - (\boldsymbol{\mu}^\top \mathbf{X}_j)^2} \mathbf{Y}_j,$$

where  $\mathbf{Y}_j, j = 1, 2, 3$  are orthogonal to  $\boldsymbol{\mu}$  and uniformly distributed on  $\mathbb{S}^{d-2}$ . So, in order to simulate  $\mathbf{X}_j$  we can easily simulate random vectors  $\mathbf{Y}_j$  and independent random variables  $\boldsymbol{\mu}^\top \mathbf{X}_j$ .

Let us find the distributions of  $\boldsymbol{\mu}^\top \mathbf{X}_j, j = 1, 2, 3$ .

**Lemma 7.1.** *The random variables  $\boldsymbol{\mu}^\top \mathbf{X}_1, \boldsymbol{\mu}^\top \mathbf{X}_2$ , and  $\boldsymbol{\mu}^\top \mathbf{X}_3$  have probability densities  $f_1, f_2$ , and  $f_3$  respectively, given by*

$$f_1(y) = \frac{2\pi^{\frac{d-1}{2}} c_{1,d}(\kappa, \alpha)}{\Gamma(\frac{d-1}{2})} \exp\left(\frac{\kappa}{\alpha} y^{<\alpha>}\right) (1 - y^2)^{\frac{d-3}{2}}, y \in [-1, 1], \quad (56)$$

$$f_2(y) = \frac{2\pi^{\frac{d-1}{2}} c_{2,d}(\kappa, \alpha)}{\Gamma(\frac{d-1}{2})} \exp\left(-\frac{\kappa}{\alpha} (1 - y)^\alpha\right) (1 - y^2)^{\frac{d-3}{2}}, y \in [-1, 1], \quad (57)$$

$$f_3(y) = \frac{2\pi^{\frac{d-1}{2}} c_{3,d}(\kappa, \alpha)}{\Gamma(\frac{d-1}{2})} \exp\left(\frac{\kappa}{\alpha} |y|^\alpha\right) (1 - y^2)^{\frac{d-3}{2}}, y \in [-1, 1]. \quad (58)$$

*Proof.* Consider  $\boldsymbol{\mu}^\top \mathbf{X}_1$ . It follows from Lemma 2.1 that

$$\begin{aligned} \mathbb{P}(\boldsymbol{\mu}^\top \mathbf{X}_1 \leq u) &= c_{1,d}(\kappa, \alpha) \int_{\|\mathbf{x}\|=1} \mathbb{1}\{\boldsymbol{\mu}^\top \mathbf{x} \leq u\} \exp\left(\frac{\kappa}{\alpha} (\boldsymbol{\mu}^\top \mathbf{x})^{<\alpha>}\right) \sigma(d\mathbf{x}) \\ &= c_{1,d}(\kappa, \alpha) \frac{2\pi^{\frac{d-1}{2}}}{\Gamma(\frac{d-1}{2})} \int_{-1}^1 \mathbb{1}\{y \leq u\} \exp\left(\frac{\kappa}{\alpha} (y)^{<\alpha>}\right) (1 - y^2)^{\frac{d-3}{2}} dy = \int_{-1}^u f_1(y) dy. \end{aligned}$$

The cases of  $\boldsymbol{\mu}^\top \mathbf{X}_2$  and  $\boldsymbol{\mu}^\top \mathbf{X}_3$  are similar.  $\square$

Applying described procedure of simulation we obtain several samples of generalized von Mises-Fisher distributions with 1000 entries on 2-dimensional sphere. For all samples we fix mean direction  $\mu = (0, \sqrt{2}/2, \sqrt{2}/2)$ . For different values of  $\alpha$  and  $\kappa$  we present locations of samples entries on a unit sphere: for Type I, see Figure 7 (with  $\alpha = 0.5$ ) and Figure 9 (with  $\alpha = 1.5$ ); for Type 2, Figures 11 and 13 with  $\alpha = 0.5$  and  $\alpha = 1.5$ , respectively, and the samples of axial data are presented in Figures 15 (with  $\alpha = 0.5$ ) and 17 (with  $\alpha = 1.5$ ). The corresponding histograms and probability densities of random variables  $\mu^T X_i, i = 1, 2, 3$  can be found in Figures 6 ( $\alpha = 0.5$ ) and 8 ( $\alpha = 1.5$ ) for Type I, in Figures 10 ( $\alpha = 0.5$ ) and 12 ( $\alpha = 1.5$ ) for Type II, and in Figures 14 ( $\alpha = 0.5$ ) and 16 ( $\alpha = 1.5$ ) for axial data.

One can observe that larger values of parameter  $\kappa$  corresponds to more concentrated samples along direction  $\mu$ .

## 7.2 Parameter estimation

We provide here a short computational study of the parameter estimation methods from sections 5.1 and 5.2. For each type of distributions GvMF<sub>1,3</sub>, GvMF<sub>2,3</sub>, GvMF<sub>3,3</sub> we simulate 1000 samples with  $N = 1000$  entries each for several values of  $\alpha \in \{0.5, 1, 1.5, 2, 2.5, 3\}$  and  $\kappa \in \{0.1, 0.5, 1, 1.5, 2, 2.5, 3, 4, 5, 6, 7\}$ . For each sample we compute maximum likelihood estimates  $\hat{\mu}_L, \hat{\alpha}_L, \hat{\kappa}_L$  and moment estimates  $\hat{\mu}_M, \hat{\alpha}_M, \hat{\kappa}_M$ . We present the sample mean square errors of  $\hat{\alpha}_L$  and  $\hat{\alpha}_M$  in Tables 7 (type I), 9 (type II), and 11 (axial type). The mean square errors of  $\hat{\kappa}_L$  and  $\hat{\kappa}_M$  can be found in Tables 8 (Type I), 10 (Type II), and 12 (axial data).

We group error values of  $\hat{\kappa}_L, \hat{\kappa}_M$  and  $\hat{\alpha}_L, \hat{\alpha}_M$  in order to decide which method is more appropriate for parameter estimation. The method of moments is preferable for Types I and II, if the computing power plays a decisive role. For axial data this method has no such advantages because we need to operate with an orientation tensor.

The experiments shows that the speed of convergence  $\hat{\alpha} \rightarrow \alpha$  and  $\hat{\kappa} \rightarrow \kappa$  depend on the values of  $\alpha$ , and  $\kappa$  and  $\hat{\kappa} \rightarrow \kappa$  faster than  $\hat{\alpha} \rightarrow \alpha$ . We can also conclude that the errors of maximum likelihood estimators are generally less than moment estimators. Comparing the errors by the distribution type, we observe that samples of Type II very often carry the smallest error.

## 7.3 Entropy estimation

In this section, we apply the  $k$ th nearest neighbour estimator (27) to the simulated set of samples. We compute estimates  $\hat{H}_{N,k}(\mathcal{X}_N)$  and their sample variances  $sVar(\hat{H}_{N,k}(\alpha, \kappa))$  for  $k = 1, 2, 3, 4, 5$ ,  $\kappa \in \{0.1, 0.5, 1, 1.5, 2, 2.5, 3, 4, 5, 6, 7\}$ , and  $\alpha \in \{0.5, 1, 1.5, 2, 2.5, 3\}$ . In Figure 1, we illustrate the distribution of  $\hat{H}_{N,k}(\mathcal{X}_N)$  with  $k = 3$  by histograms for samples simulated from distributions GvMF <sub>$j,3$</sub> (1.5, 2, ·),  $j = 1, 2, 3$ .

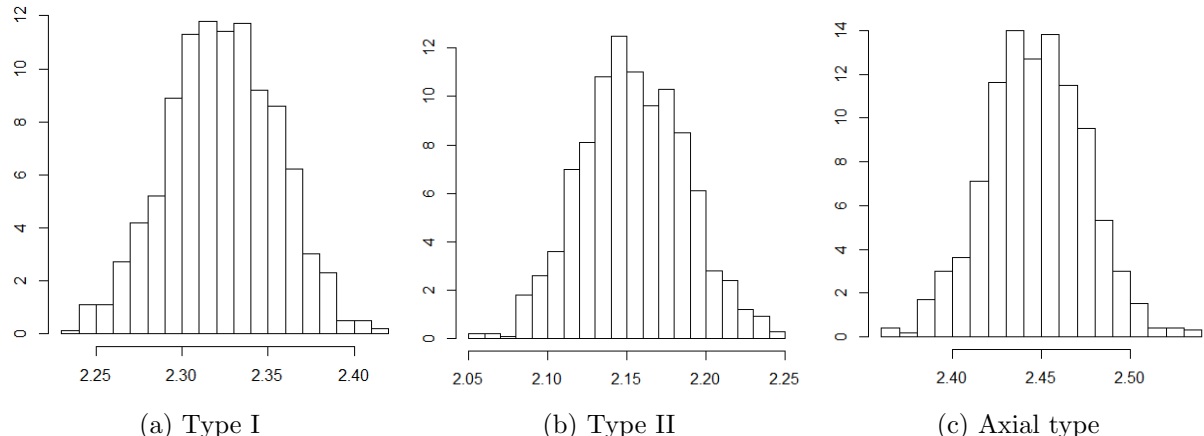


Figure 1: Histograms of  $\hat{H}_{N,3}(\mathcal{X}_N)$ ,  $\mathcal{X}_N \sim \text{GvMF}_{j,3}(\alpha, \kappa, \cdot)$  with  $\alpha = 1.5$  and  $\kappa = 2$ .

In order to choose the right value of  $k$  we compare the sample variances  $sVar(\hat{H}_{N,k}(\alpha, \kappa))$  for  $k = 1, 2, 3, 4, 5$ . The minimum and maximum values of  $sVar(\hat{H}_{N,k}(\alpha, \kappa))$  with respect to  $\alpha$  and  $\kappa$  are presented in Table 1. Our results confirm the conclusion in (Berrett et al., 2019), that is, the asymptotic variance

of  $\hat{H}_{N,k}$  decreases rapidly up to  $k = 3$ . One can observe that  $k$ -nearest neighbour estimates depend on values  $\alpha$  and  $\kappa$ . Although, the sample variances are quite small for all examined values of  $\alpha$  and  $\kappa$  and sample size  $N = 1000$ .

Distribution		$k = 1$	$k = 2$	$k = 3$	$k = 4$	$k = 5$
$GvMF_{1,3}(\alpha, \kappa)$	$\min_{\alpha, \kappa}(sVar)$	0.00214	0.00092	0.00058	0.00042	0.00034
	$\max_{\alpha, \kappa}(sVar)$	0.00388	0.00239	0.00208	0.00185	0.00152
$GvMF_{2,3}(\alpha, \kappa)$	$\min_{\alpha, \kappa}(sVar)$	0.00212	0.00093	0.00059	0.00043	0.00034
	$\max_{\alpha, \kappa}(sVar)$	0.00404	0.00304	0.00275	0.00152	0.00257
$GvMF_{3,3}(\alpha, \kappa)$	$\min_{\alpha, \kappa}(sVar)$	0.00212	0.00093	0.00059	0.00043	0.00034
	$\max_{\alpha, \kappa}(sVar)$	0.00334	0.00207	0.00170	0.00152	0.00144

Table 1: Sample variance  $sVar(\hat{H}_{N,k}(\alpha, \kappa))$  for distribution of type I

Thus, we choose  $k = 3$  for computations in the next sections.

## 7.4 Test statistic

In this section, we present our study of the goodness of fit tests from Section 6 and their test statistics  $\hat{T}_{j,k}(\mathcal{X}_N)$ ,  $j = 1, 2, 3$  from (53), (54) and (55) with  $k = 3$  and  $N = 1000$ . We compute  $\hat{T}_{j,k}^L(\mathcal{X}_N)$  and  $\hat{T}_{j,k}^M(\mathcal{X}_N)$  separately with maximum likelihood estimates and estimates by the method of moments of parameters  $\alpha, \kappa, \mu$ , respectively.

For comparison of different types of estimates, we look on the sample variances  $sVar(\hat{T}_{j,3}^M(\alpha, \kappa))$  and  $sVar(\hat{T}_{j,3}^L(\alpha, \kappa))$  of  $\hat{T}_{j,3}^M(\mathcal{X}_N)$  and  $\hat{T}_{j,3}^L(\mathcal{X}_N)$ , respectively, for all combinations of parameters  $\kappa \in \{0.1, 0.5, 1, 1.5, 2, 2.5, 3, 4, 5, 6, 7\}$  and  $\alpha \in \{0.5, 1, 1.5, 2, 2.5, 3\}$ . The minimum and maximum values of  $sVar(\hat{T}_{j,3}^M(\alpha, \kappa))$  and  $sVar(\hat{T}_{j,3}^L(\alpha, \kappa))$  are presented in Table 2. Numbers in this tables demonstrate significant benefits of the maximum likelihood method over the method of moments for distributions of I and II types. For axial data, one can also prefer  $\hat{T}_{j,k}^L$ . Additionally, one can observe from Table 2 and tables with errors of estimates  $\hat{\kappa}^L, \hat{\kappa}^M, \hat{\alpha}^L, \hat{\alpha}^M$  that the statistics  $\hat{T}_{j,k}^M$  and  $\hat{T}_{j,k}^L$  are much more accurate than estimators of parameters and they have small variances even for small  $\alpha, \kappa$  in contrast to  $\hat{\alpha}, \hat{\kappa}$ , whose deviations are large.

In Section 6, we choose the two-sided test with rejection criteria  $|\hat{T}_{j,k}^L| > x_{\beta,j}$ . We confirm this choice by histograms  $\hat{T}_{j,3}^L$  with  $\alpha = 1.5$  and  $\kappa = 2$ , see Figure 2.

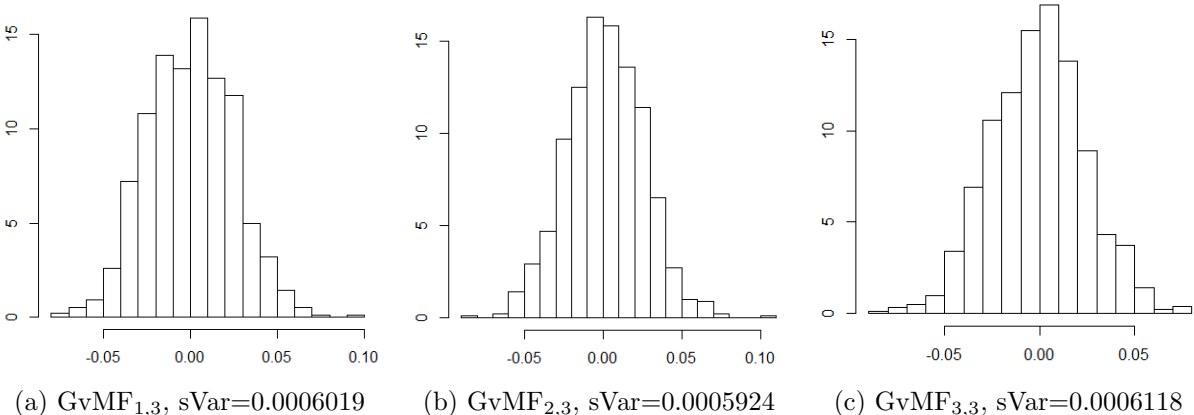


Figure 2: Histograms of  $\hat{T}_{j,3}^L(\mathcal{X}_N)$ ,  $\mathcal{X}_N \sim GvMF_{j,3}(\alpha, \kappa, \cdot)$  with  $\alpha = 1.5$  and  $\kappa = 2$ .

Type of estimates	Moments			Maximum likelihood		
	$GvMF_{1,3}$	$GvMF_{2,3}$	$GvMF_{3,3}$	$GvMF_{1,3}$	$GvMF_{2,3}$	$GvMF_{3,3}$
$\min_{\alpha, \kappa}(sVar)$	0.000563	0.000538	0.000573	0.000558	0.000535	0.000544
$\max_{\alpha, \kappa}(sVar)$	0.001014	0.001558	0.000734	0.000665	0.000688	0.000667

Table 2: Sample variances  $sVar(\hat{T}_{j,3}^L(\alpha, \kappa))$

We see that the statistics  $\hat{T}_{j,3}^L$  have approximately symmetric distribution with mode at 0. Therefore, we put rejection region as  $(-\infty, -x_\beta) \cup [x_\beta, +\infty)$ , where critical values  $x_\beta$  are obtained as a samples quantiles  $\mathbb{P}_{H_0}(|\hat{T}_{i,3}| > x_{\beta,j}) \leq \beta, j = 1, 2, 3$ . The corresponding values of  $x_{\beta,j}$  with significance level  $\beta = 0.05$  are presented in Table 3 for  $\hat{T}_{1,3}^L$ , in Table 4 for  $\hat{T}_{2,3}^L$ , and in Table 5 for  $\hat{T}_{3,3}^L$ .

	0.1	0.5	1	1.5	2	2.5	3	4	5	6	7
0.5	4.884	4.626	5.128	5.281	5.069	4.960	4.726	4.999	5.132	5.360	5.301
1	4.727	4.792	4.879	4.736	4.757	4.843	4.920	5.217	4.951	5.278	5.091
1.5	4.935	4.914	4.657	4.731	4.745	4.879	4.849	4.995	5.152	4.990	5.009
2	4.916	4.873	4.839	4.982	4.801	4.987	4.752	4.934	4.829	5.076	5.010
2.5	4.916	4.921	5.276	4.932	4.854	4.852	4.711	4.700	4.860	4.983	5.373
3	4.687	4.821	4.783	4.626	4.926	4.704	4.656	4.690	4.631	4.706	4.844

Table 3: Critical values  $x_{\beta,1}$  for test statistic  $\hat{T}_{1,3}^L$  and  $\beta = 0.05$ , with respect to  $\alpha$  (rows) and  $\kappa$  (columns), multiplied by  $10^2$ .

	0.1	0.5	1	1.5	2	2.5	3	4	5	6	7
0.5	4.921	4.795	4.750	4.962	4.711	5.015	4.742	5.182	5.430	5.374	5.388
1	4.718	4.688	4.858	4.937	4.996	4.829	4.870	5.065	5.234	5.287	5.449
1.5	4.698	4.916	4.943	4.714	4.824	4.988	4.964	4.613	4.975	5.267	5.263
2	4.920	4.989	4.852	4.611	4.890	4.869	5.147	5.037	4.941	5.423	5.217
2.5	5.066	4.753	5.034	4.805	4.768	4.930	4.973	5.346	5.283	5.138	5.074
3	4.713	4.417	4.731	4.907	5.001	5.007	4.870	5.023	5.015	5.083	5.116

Table 4: Critical values  $x_{\beta,2}$  for test statistic  $\hat{T}_{2,3}^L$  and  $\beta = 0.05$ , with respect to  $\alpha$  (rows) and  $\kappa$  (columns), multiplied by  $10^2$ .

	0.1	0.5	1	1.5	2	2.5	3	4	5	6	7
0.5	4.932	5.095	4.843	4.863	5.040	4.995	5.000	5.477	5.810	5.219	5.527
1	4.956	4.793	4.636	4.912	4.896	4.873	4.959	5.251	5.196	5.565	5.917
1.5	4.620	4.873	4.781	4.892	4.839	5.006	4.806	4.824	5.016	5.239	5.370
2	4.727	5.049	4.804	4.567	4.811	4.651	4.842	4.999	4.836	5.162	5.191
2.5	4.925	4.799	4.938	4.831	4.735	4.834	5.024	4.739	4.917	4.899	4.703
3	4.960	4.901	4.904	4.649	5.037	4.843	4.898	4.852	4.828	4.895	4.974

Table 5: Critical values  $x_{\beta,3}$  for test statistic  $\hat{T}_{3,3}^L$  and  $\beta = 0.05$ , with respect to  $\alpha$  (rows) and  $\kappa$  (columns), multiplied by  $10^2$ .

We provide also the study of the goodness of fit test's power for the samples from Fisher-Bingham distribution. We put  $\mu_1 = (1, 0, 0)^T$  and  $\mu_2 = (0, \sqrt{2}/2, \sqrt{2}/2)^T$  and consider the following series of hypotheses.

For type I:

- $H_0^1 : \mathbf{X} \sim \text{GvMF}_{1,3}$ ,
- $H_{1,j}^1 : \mathbf{X}$  has the Fisher-Bingham distribution with density  $\propto \exp(3\mu_1^T \mathbf{x} + 0.35j(\mu_2^T \mathbf{x})^2)$ ,  $\mathbf{x} \in \mathbb{S}^2$ ,  $j = 1, \dots, 20$ .

For axial type:

- $H_0^2 : \mathbf{X} \sim \text{GvMF}_{3,3}$ ,
- $H_{1,j}^2 : \mathbf{X}$  has the Fisher-Bingham distribution with density  $\propto \exp(0.05j(\mu_1^T \mathbf{x}) + 6(\mu_2^T \mathbf{x})^2)$ ,  $\mathbf{x} \in \mathbb{S}^2$ ,  $j = 1, \dots, 20$ .

For each  $j = 1, \dots, 20$ , we simulate 500 samples  $\mathcal{X}_{j,N}^1$  under  $H_{1,j}^1$  and  $\mathcal{X}_{j,N}^2$  under  $H_{1,j}^2$  with sample size  $N = 1000$ . We use the simulation procedure from the R package ‘Directional’ (Tsagris et al., 2020). In order to simplify commutations, we reject  $H_0^1$  and  $H_0^2$  if  $|\hat{T}_{1,3}^L(\mathcal{X}_{j,N}^1)| > x_\beta^{(1)}$  and  $|\hat{T}_{2,3}^L(\mathcal{X}_{j,N}^2)| > x_\beta^{(2)}$  respectively, where critical values  $x_\beta^{(1)} = 0.05373$  and  $x_\beta^{(2)} = 0.05917$  are taken as maximum of  $x_\beta$  from Tables 3 and 5 for significance level  $\beta = 0.05$ .

The ratios of rejections  $H_0^1$  and  $H_0^2$  are presented in Figure 3.

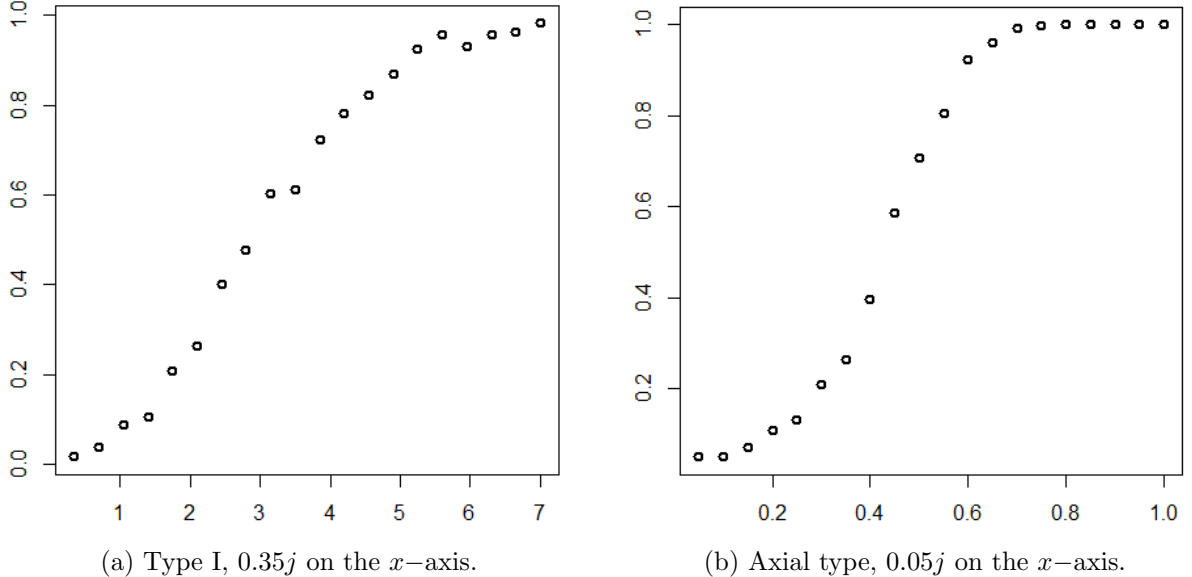


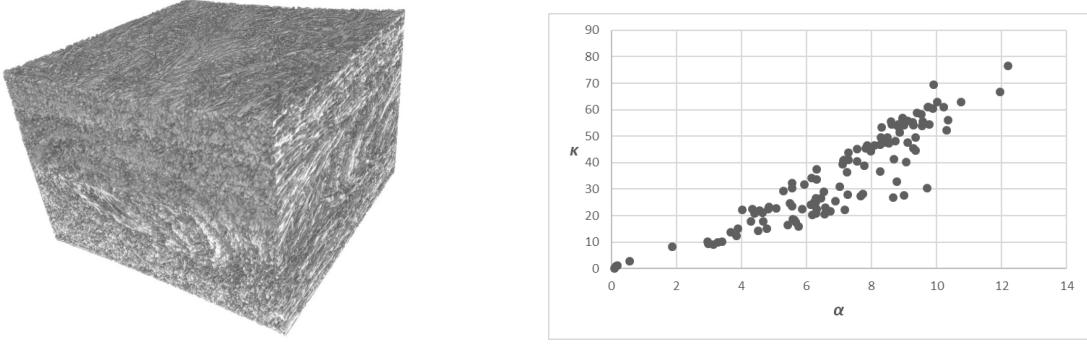
Figure 3: Powers of goodness of fit tests  $H_0^1$  vs  $H_{1,j}^1$  (left) and  $H_0^2$  vs  $H_{1,j}^2$  (right),  $j = 1, \dots, 20$ .

## 8 Application to a real data set

In this section, we apply the introduced goodness of fit test to the data set consists of fiber directions in a glass fibre reinforced composite material. The 3D-images of a fibre composite obtained by micro computed tomography and are provided by the Institute for Composite Materials (IVW) in Kaiserslautern, Germany, see Fig. 4b (left). The detailed description of the material can be found in (Wirjadi et al., 2014) and it was the object of studies in (Dresvyanskiy et al., 2019) and (Dresvyanskiy et al., 2020), where the regions of anomaly behaviour of the fibres were found. The data set is provided by Prof. Claudia Redenbach (TU Kaiserslautern) and consists of local direction of fibres estimated by the tools of MAVI software (Fraunhofer ITWM, Department of Image Processing, 2005). Each data set entry  $Y_k, k = ([1, 97] \times [1, 80] \times [1, 64]) \cap \mathbb{N}^3$  is the average of fibre local directions in small observation windows  $W$  with  $75 \times 75 \times 75$  voxels each. Note that some of such windows can be empty or they might contain not enough material for direction computation. We denote by  $J_W$  the collection of indexes  $k$  such that  $Y_k$  is non-empty. In the considered data set  $|J_W| = 430741$  and its precise construction is in (Dresvyanskiy et al., 2019).

The estimating procedure of directions in MAVI software produces vectors on a unit sphere which are not necessarily symmetrically distributed. However, the fibres are not oriented, therefore we expect an axial distribution of their directions. We propose the symmetrization of original sample by  $\mathcal{X}_N = \{\mathbf{X}_k = \mathbf{Y}_k \xi_k, \mathbf{k} \in J_W\}$ , where  $\xi_k, \mathbf{k} \in J_W$  are i.i.d random variables with  $\mathbb{P}(\xi_k = +1) = \mathbb{P}(\xi_k = -1) = \frac{1}{2}$ . We separate the whole material into blocks  $W_1$ , each of size  $16 \times 15 \times 16$ , such that  $J_1 = J_W \cap [l_1, l_1 + 16] \times [l_2, l_2 + 15] \times [l_3, l_3 + 16]$  and consider subsamples  $\mathcal{X}_1 = \{\mathbf{X}_k, \mathbf{k} \in J_1\}$  with simple sizes  $2736 \leq |\mathcal{X}_1| \leq 3745$ . For each subsample  $\mathcal{X}_1$  we provide the introduced goodness of fit test for distributions  $\text{GvMF}_{3,3}$ , i.e., we test

- $H_{0,1} : \mathcal{X}_1 \sim \text{GvMF}_{3,3}$
- $H_{1,1} : \mathcal{X}_1 \not\sim \text{GvMF}_{3,3}$ .



(a) 3D image of a glass fibre reinforced composite material. 970×1469×1217 voxels, spacing: for each subsample  $\mathcal{X}_l$  4 $\mu\text{m}$ . (b) Maximum likelihood estimates of  $\alpha$  and  $\kappa$  for each subsample  $\mathcal{X}_l$

Figure 4: Testing on glass fibre reinforced composite material.

At first, we provide maximum likelihood estimation of parameters  $\alpha$  and  $\kappa$  (for the variety of their values  $\hat{\alpha}_l$  and  $\hat{\kappa}_l$  see Figure 4b). Second, we need to simulate the samples of statistics  $\hat{T}_{3,k}(\mathcal{X}_l)$  under hypotheses  $\mathcal{X}_l \sim \text{GvMF}_{3,3}(\hat{\alpha}_l, \hat{\kappa}_l, \cdot)$  based on samples sizes  $|\mathcal{X}_l|$ . Unfortunately, our computational resources was limited and we have to group simulations with close values of  $\hat{\alpha}_l$  and  $\hat{\kappa}_l$ . One can observe that the majority of  $\hat{\alpha}_l$  belongs to the interval [3, 11] and the ratios  $\frac{\hat{\kappa}_l}{\hat{\alpha}_l}$  are mostly in [3, 7]. Therefore, we simulate 800 samples  $\mathcal{Y}_N \sim \text{GvMF}_{3,3}(\alpha, \kappa, \cdot)$  each of size  $N = 3500$  for all combinations of  $\alpha \in \{4, 6, 8, 10\}$  and  $\frac{\kappa}{\alpha} \in \{4, 6\}$  to obtain the corresponding empirical distributions of  $\hat{T}_{3,3}(\mathcal{Y}_N)$ .

Then we compute statistics  $\hat{T}_{3,3}(\mathcal{X}_l)$  for each  $l$  and their  $p$ -values. We obtain that our goodness of fit test rejects almost all hypotheses  $H_{0,l}$  with significance level 0.05, and detects 3 regions with directional distributions GvMF<sub>3,3</sub> (see Table 6 for the samples  $\mathcal{X}_l$  with  $p$ -values greater than 0.01). In order to illustrate how tight the fitted distributions are, we present for two blocks  $W_l$  with  $l = (49, 61, 1)$  and  $l = (49, 61, 1)$ , the QQ-plots for samples  $\{\hat{\mu}_l^T \mathbf{X}_k\}$  and distribution  $f_3$  defined in (58) with parameters  $(\hat{\alpha}_l, \hat{\kappa}_l, \cdot)$ , see Figure 5.

$l_1$	$l_2$	$l_3$	$ \mathcal{X}_l $	$\hat{\mu}$	$\hat{\alpha}$	$\hat{\kappa}$	$\hat{H}_{N,3}$	$\hat{T}_{3,3}(\mathcal{X}_l)$	$p$ -value
49	46	1	3434	(-0.0028, 0.9999, -0.0135)	8.80	53.90	0.4369	0.02344	0.0775
49	61	1	3222	(-0.0149, 0.9998, 0.0091)	8.53	47.62	0.7132	0.01976	0.1234
49	16	17	3474	(0.0175, 0.9977, 0.0657)	8.84	53.63	0.4690	0.02987	0.0263
49	61	17	3364	(-0.0125, 0.9998, -0.0152)	10.22	60.91	0.4628	0.02946	0.0263
1	46	65	3319	(-0.0297, 0.9986, -0.0432)	7.25	36.45	1.0455	0.02057	0.1275

Table 6: Results of goodness of fit tests  $H_{0,l}$  vs.  $H_{1,l}$  for fiber directions in glass fibre reinforced composite material.

## Acknowledgement

The research was partially supported by DFG Grant 390879134. The authors are grateful for Prof. Katja Schladitz for the help with the real data, Martin Gurka and Sebastian Nissle (Institut für Verbundwerkstoffe, Kaiserslautern) for permission to reuse the tomographic images, Prof. Claudia Redenbach for providing the data set of fiber directions.

## References

- BERGER, M. & GOSTIAUX, B. (1988). *Differential geometry: manifolds, curves, and surfaces*, vol. 115 of *Graduate Texts in Mathematics*. Springer-Verlag, New York. Translated from the French by Silvio Levy.

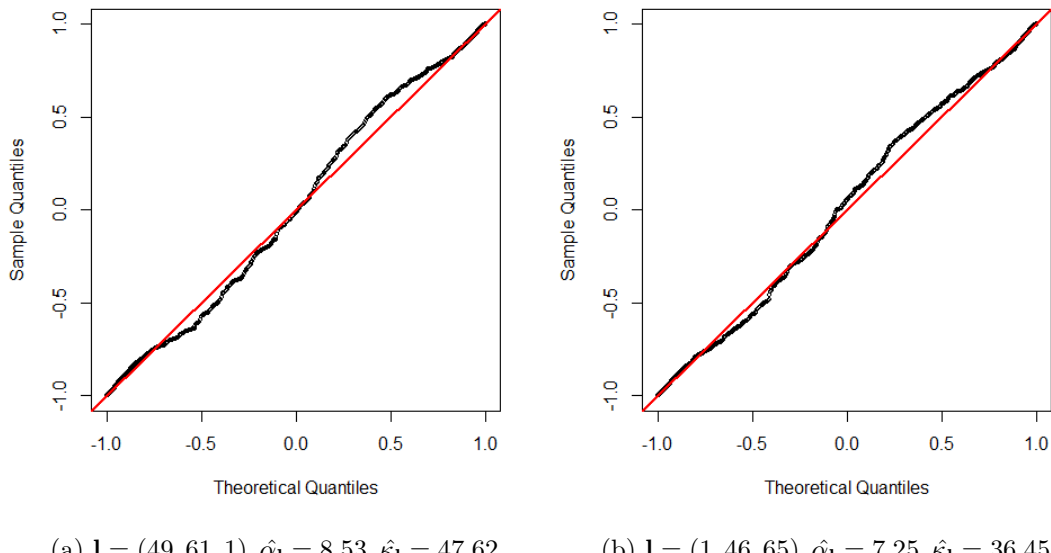


Figure 5: QQ plots for samples  $\hat{\mu}_l^T \mathbf{X}_l$  and distributions with density  $f_3$  (58).

BERRETT, T. B. & SAMWORTH, R. J. (2019). Nonparametric independence testing via mutual information. *Biometrika* **106**, 547–566.

BERRETT, T. B., SAMWORTH, R. J. & YUAN, M. (2019). Efficient multivariate entropy estimation via  $k$ -nearest neighbour distances. *Ann. Statist.* **47**, 288–318.

BINGHAM, M. & MARDIA, K. (1975). Maximum likelihood characterization of the von Mises distribution. In *A Modern Course on Statistical Distributions in Scientific Work*. Springer, pp. 387–398.

BULINSKI, A. & DIMITROV, D. (2019). Statistical estimation of the Shannon entropy. *Acta Math. Sin. (Engl. Ser.)* **35**, 17–46.

CADIRCI, M. S., EVANS, D., LEONENKO, N. & MAKOGIN, V. (2020). Entropy-based test for generalized Gaussian distributions. ArXiv preprint arXiv:2010.06284.

DELATTRE, S. & FOURNIER, N. (2017). On the Kozachenko-Leonenko entropy estimator. *J. Statist. Plann. Inference* **185**, 69–93.

DRESVYANSKIY, D., KARASEVA, T., MAKOGIN, V., MITROFANOV, S., REDENBACH, C. & SPODAREV, E. (2020). Detecting anomalies in fibre systems using 3-dimensional image data. *Statistics and Computing* , 1–21.

DRESVYANSKIY, D., KARASEVA, T., MITROFANOV, S., REDENBACH, C., SCHWAAR, S., MAKOGIN, V. & SPODAREV, E. (2019). Application of clustering methods to anomaly detection in fibrous media. *IOP Conference Series: Materials Science and Engineering* **537**, 022001.

EVANS, D. (2008). A law of large numbers for nearest neighbour statistics. *Proc. R. Soc. Lond. Ser. A Math. Phys. Eng. Sci.* **464**, 3175–3192.

EVANS, D., JONES, A. J. & SCHMIDT, W. M. (2002). Asymptotic moments of near-neighbour distance distributions. *R. Soc. Lond. Proc. Ser. A Math. Phys. Eng. Sci.* **458**, 2839–2849.

FANG, K. T. & ZHANG, Y. T. (1990). *Generalized Multivariate Analysis*. Springer-Verlag, Berlin; Science Press Beijing, Beijing.

FRAUNHOFER ITWM, DEPARTMENT OF IMAGE PROCESSING (2005). MAVI – modular algorithms for volume images. <http://www.mavi-3d.de>.

- GAO, W., OH, S. & VISWANATH, P. (2018). Demystifying fixed  $k$ -nearest neighbor information estimators. *IEEE Trans. Inform. Theory* **64**, 5629–5661.
- GATTO, R. & JAMMALAMADKA, S. R. (2007). The generalized von Mises distribution. *Stat. Methodol.* **4**, 341–353.
- GORIA, M. N., LEONENKO, N. N., MERGEL, V. V. & NOVI INVERARDI, P. L. (2005). A new class of random vector entropy estimators and its applications in testing statistical hypotheses. *J. Nonparametr. Stat.* **17**, 277–297.
- KOZACHENKO, L. F. & LEONENKO, N. N. (1987). Sample estimate of the entropy of a random vector. *Problems of Information Transmission* **23**, 95–101.
- LEONENKO, N., PRONZATO, L. & SAVANI, V. (2008). A class of Rényi information estimators for multidimensional densities. *Ann. Statist.* **36**, 2153–2182. Corrected by Leonenko, N. and Pronzato, L. Correction: A class of Rényi information estimators for multidimensional densities. *Ann. Statist.* **38**, 3837–3838.
- LI, S., MNATSAKANOV, R. M. & ANDREW, M. E. (2011).  $k$ -nearest neighbor based consistent entropy estimation for hyperspherical distributions. *Entropy* **13**, 650–667.
- LUND, U. & JAMMALAMADKA, S. R. (2000). An entropy-based test for goodness of fit on the von Mises distribution. *J. Statist. Comput. Simulation* **67**, 319–332.
- LUTWAK, E., YANG, D. & ZHANG, G. (2004). Moment-entropy inequalities. *Ann. Probab.* **32**, 757–774.
- MARDIA, K. V. (1975). Statistics of directional data. *J. Roy. Statist. Soc. Ser. B* **37**, 349–393.
- MARDIA, K. V. & JUPP, P. E. (2000). *Directional Statistics*. Wiley Series in Probability and Statistics. John Wiley & Sons, Ltd., Chichester.
- MISRA, N., SINGH, H. & HNIZDO, V. (2010). Nearest neighbor estimates of entropy for multivariate circular distributions. *Entropy* **12**, 1125–1144.
- MOURITSEN, H. & MOURITSEN, O. (2000). A mathematical expectation model for bird navigation based on the clock-and-compass strategy. *Journal of Theoretical Biology* **207**, 283 – 291.
- PENROSE, M. D. & YUKICH, J. E. (2013). Limit theory for point processes in manifolds. *Ann. Appl. Probab.* **23**, 2161–2211.
- PISCHIUTTA, M., ROVELLI, A., SALVINI, F., DI GIULIO, G. & BEN-ZION, Y. (2013). Directional resonance variations across the Pernicana Fault, Mt Etna, in relation to brittle deformation fields. *Geophysical Journal International* **193**, 986–996.
- SHABANI, B., BABANIN, A. V. & BALDOCK, T. E. (2016). Observations of the directional distribution of the wind energy input function over swell waves. *Journal of Geophysical Research: Oceans* **121**, 1174–1193.
- TORRANCE, K. E., SPARROW, E. M. & BIRKEBAK, R. C. (1966). Polarization, directional distribution, and off-specular peak phenomena in light reflected from roughened surfaces. *J. Opt. Soc. Am.* **56**, 916–925.
- TSAGRIS, M., ATHINEOU, G., SAJIB, A., AMSON, E. & WALDSTEIN, M. J. (2020). *Directional: Directional Statistics*. R package version 4.4.
- WIRJADI, O., GODEHARDT, M., SCHLADITZ, K., WAGNER, B., RACK, A., GURKA, M., NISSLER, S. & NOLL, A. (2014). Characterization of multilayer structures of fiber reinforced polymer employing synchrotron and laboratory X-ray CT. *International Journal of Materials Research* **105**, 645–654.
- WYATT, L. R., LEDGARD, L. J. & ANDERSON, C. W. (1997). Maximum-Likelihood Estimation of the Directional Distribution of 0.53-Hz Ocean Waves. *Journal of Atmospheric and Oceanic Technology* **14**, 591–603.
- YUKICH, J. E. (2006). *Probability Theory of Classical Euclidean Optimization Problems*. Springer.

## Appendix

Here we present tables of mean square errors of estimates of  $\kappa$  and  $\alpha$  and plots with realisations of the generalized von Mises-Fisher distributions

	0.1	0.5	1	1.5	2	2.5	3	4	5	6	7
0.5	2.03233	0.01131	0.00309	0.00229	0.00334	0.00720	0.00234	0.00067	0.00044	0.00046	0.00040
	1.74912	0.01103	0.00294	0.00209	0.00290	0.00600	0.01028	0.01568	0.02000	0.02222	0.02375
	12.64360	0.27260	0.03760	0.01778	0.01126	0.00766	0.00633	0.00686	0.00950	0.02210	0.04043
1	15.83364	0.21929	0.03207	0.01518	0.00838	0.00569	0.00480	0.00508	0.00644	0.00850	0.01633
	13.64093	2.89363	0.44954	0.12728	0.07166	0.04616	0.03330	0.02049	0.01535	0.01465	0.01516
	24.85928	2.75421	0.20300	0.07216	0.03613	0.02355	0.01725	0.01081	0.00904	0.00793	0.00854
1.5	12.95277	8.34069	2.90354	0.89834	0.44383	0.27728	0.16970	0.08593	0.05445	0.04011	0.03321
	26.53262	10.16847	1.30990	0.30051	0.13914	0.08601	0.05726	0.03554	0.02187	0.01650	0.01406
	11.71910	8.68665	6.79656	3.96727	2.18844	1.23084	0.62982	0.35996	0.18528	0.13112	0.09397
2	26.53403	15.44292	4.46642	1.21787	0.42840	0.23206	0.16395	0.08478	0.05083	0.03633	0.02807
	11.23635	10.18631	8.74483	6.31636	6.33024	3.48461	2.84763	1.35829	0.62283	0.50274	0.33681
	23.03320	18.71290	8.33385	3.35711	1.24416	0.60680	0.36062	0.20265	0.11569	0.08699	0.05869

Table 7: Mean square errors of  $\hat{\alpha}_M$  (top raw) and  $\hat{\alpha}_L$  (bottom raw) for GvMF<sub>1,3</sub> distribution, for different values of  $\alpha$  (rows) and  $\kappa$  (columns)

	0.1	0.5	1	1.5	2	2.5	3	4	5	6	7
0.5	0.71826	0.01899	0.01699	0.01898	0.02602	0.03563	0.03419	0.03749	0.04394	0.06683	0.07928
	0.37326	0.01717	0.01598	0.01727	0.02396	0.03306	0.04987	0.07889	0.10651	0.13889	0.17365
	1.94226	0.22319	0.07076	0.06534	0.06965	0.06449	0.06737	0.08770	0.11201	0.19431	0.31639
1	2.46363	0.11194	0.05895	0.05552	0.05215	0.05029	0.05277	0.06947	0.08617	0.10606	0.16075
	1.53572	2.11049	0.64790	0.26637	0.25165	0.23415	0.22145	0.20812	0.20797	0.23012	0.24837
	3.63032	1.19008	0.19097	0.14496	0.12205	0.11508	0.11355	0.10874	0.12384	0.12786	0.14523
1.5	1.58362	3.68444	4.15468	1.72159	1.18887	1.05376	0.82951	0.63399	0.54231	0.49912	0.52341
	3.87311	3.19240	0.92650	0.39620	0.29374	0.27322	0.24016	0.24388	0.20779	0.19860	0.21512
	1.34224	2.17772	6.54718	7.27056	5.81158	4.41608	2.47149	2.26686	1.43704	1.34411	1.22740
2	4.13401	4.02490	2.52365	1.19600	0.61967	0.50278	0.50154	0.41390	0.35365	0.35024	0.33833
	1.08917	1.87215	5.16488	7.11001	13.3072	10.1227	11.0565	7.43739	4.25858	4.56458	3.74400
	3	3.97375	4.29139	3.63187	2.47833	1.40486	0.99006	0.80562	0.74920	0.62553	0.61910

Table 8: Mean square error of  $\hat{\kappa}_M$  (top raw) and  $\hat{\kappa}_L$  (bottom raw) for GvMF<sub>1,3</sub> distribution, for different values of  $\alpha$  (rows) and  $\kappa$  (columns)

	0.1	0.5	1	1.5	2	2.5	3	4	5	6	7
0.5	2.15430	0.04439	0.00892	0.00384	0.00240	0.00200	0.00176	0.00174	0.00208	0.00112	0.00053
	4.05118	0.03719	0.00571	0.00244	0.00131	0.00111	0.00082	0.00069	0.00073	0.00072	0.00079
	2.43731	0.11476	0.02662	0.01238	0.00779	0.00620	0.00508	0.00415	0.00424	0.00384	0.00421
1	6.35329	0.15498	0.02641	0.01200	0.00721	0.00555	0.00469	0.00369	0.00357	0.00341	0.00369
	2.82117	0.20015	0.05429	0.02785	0.01742	0.01432	0.01291	0.00981	0.00956	0.00925	0.01026
	8.76630	0.30670	0.05952	0.02937	0.01765	0.01473	0.01303	0.01006	0.01004	0.00962	0.01057
1.5	2.55262	0.30415	0.09795	0.05169	0.03786	0.02962	0.02579	0.02137	0.02306	0.02314	0.02297
	9.04940	0.40585	0.09406	0.05020	0.03618	0.02640	0.02466	0.01993	0.02191	0.02198	0.02143
	2.27668	0.56165	0.12324	0.08668	0.06643	0.05643	0.05414	0.05298	0.04757	0.05055	0.04818
2	8.21909	0.51124	0.12344	0.06832	0.05349	0.04539	0.04304	0.04235	0.03748	0.04087	0.03752
	2.64239	0.71927	0.18736	0.14068	0.11660	0.11100	0.11534	0.09450	0.10280	0.10102	0.10246
	8.45839	0.52430	0.16199	0.09598	0.08051	0.07280	0.07200	0.06493	0.07062	0.06307	0.06369

Table 9: Mean square error of  $\hat{\alpha}_M$  (top raw) and  $\hat{\alpha}_L$  (bottom raw) for GvMF<sub>2,3</sub> distribution, for different values of  $\alpha$  (rows) and  $\kappa$  (columns)

	0.1	0.5	1	1.5	2	2.5	3	4	5	6	7
0.5	0.00308	0.00593	0.00788	0.01080	0.01751	0.03210	0.05088	0.14597	0.39689	0.26720	0.11059
	0.00264	0.00585	0.00619	0.00815	0.01132	0.02080	0.02932	0.06803	0.16595	0.29599	0.54081
	0.00290	0.00460	0.00611	0.00912	0.01508	0.02487	0.03871	0.08568	0.18878	0.31815	0.56937
	0.00299	0.00504	0.00602	0.00885	0.01432	0.02260	0.03695	0.07654	0.16276	0.28533	0.50945
	0.00317	0.00382	0.00496	0.00712	0.01159	0.02027	0.03192	0.07540	0.16707	0.28675	0.52890
	0.00352	0.00433	0.00497	0.00715	0.01170	0.02050	0.03221	0.07713	0.17453	0.29832	0.54837
1.5	0.00312	0.00507	0.00512	0.00658	0.01078	0.01733	0.02968	0.07776	0.17039	0.33426	0.54030
	0.00379	0.00594	0.00515	0.00663	0.01090	0.01729	0.02992	0.07590	0.16294	0.32125	0.52428
	0.00298	0.00725	0.00705	0.00885	0.01145	0.01878	0.03171	0.08975	0.19040	0.36456	0.65539
	0.00411	0.00797	0.00761	0.00847	0.01155	0.01850	0.03021	0.07865	0.16314	0.29699	0.52800
	0.00277	0.01072	0.01052	0.01256	0.01447	0.02044	0.03274	0.09333	0.24011	0.45512	0.87428
	0.00449	0.01004	0.01033	0.01179	0.01420	0.02058	0.03070	0.07711	0.17748	0.30782	0.52693

Table 10: Mean square error of  $\hat{\kappa}_M$  (top raw) and  $\hat{\kappa}_L$  (bottom raw) for GvMF<sub>2,3</sub> distribution, for different values of  $\alpha$  (rows) and  $\kappa$  (columns)

	0.1	0.5	1	1.5	2	2.5	3	4	5	6	7
0.5	2.29602	0.18987	0.05705	0.02550	0.01188	0.00814	0.00512	0.00236	0.00128	0.00045	0.00045
	3.79114	0.16463	0.04162	0.02490	0.01907	0.01631	0.01637	0.02073	0.02427	0.02521	0.02548
	1.89494	0.72857	0.23713	0.11809	0.07490	0.05300	0.03753	0.02852	0.01925	0.01203	0.00443
	6.47041	1.99071	0.21501	0.08130	0.04956	0.03309	0.02432	0.02189	0.01923	0.02272	0.02594
	2.09251	1.41746	0.69305	0.28007	0.16580	0.09577	0.07204	0.04872	0.03733	0.03224	0.02760
	12.7767	7.55889	1.11221	0.28031	0.14598	0.08200	0.06144	0.04110	0.03296	0.02763	0.02579
1.5	2.18619	2.16193	1.34087	0.66370	0.37039	0.20955	0.15980	0.09065	0.05605	0.04741	0.03871
	18.4855	11.8352	4.29336	1.22665	0.40504	0.20974	0.16143	0.08807	0.05484	0.04622	0.03623
	3.15268	3.14653	2.42570	1.51950	0.79157	0.47397	0.33253	0.17312	0.11837	0.08002	0.06680
	20.7207	17.0535	7.75701	3.11424	1.16675	0.52106	0.34421	0.18537	0.12071	0.08197	0.06698
	4.56639	4.87133	4.04307	2.64681	1.72811	1.07167	0.70276	0.33226	0.20734	0.15167	0.11787
	20.2178	17.9717	10.7576	5.75811	2.78415	1.28941	0.74024	0.35797	0.22610	0.15511	0.12132

Table 11: Mean square error of  $\hat{\alpha}_M$  (top raw) and  $\hat{\alpha}_L$  (bottom raw) for GvMF<sub>3,3</sub> distribution, for different values of  $\alpha$  (rows) and  $\kappa$  (columns)

	0.1	0.5	1	1.5	2	2.5	3	4	5	6	7
0.5	0.29970	0.06602	0.05435	0.05186	0.04292	0.04582	0.04249	0.05097	0.05318	0.06447	0.08802
	0.60213	0.06010	0.04156	0.04885	0.05101	0.05939	0.06571	0.10154	0.12560	0.15621	0.18777
	0.19968	0.14994	0.12997	0.13578	0.14216	0.14670	0.12929	0.14336	0.14140	0.14276	0.10894
	0.89717	0.64104	0.14258	0.10734	0.10834	0.10368	0.09266	0.11498	0.12950	0.17055	0.19490
	0.18726	0.22813	0.22610	0.21028	0.22102	0.19741	0.19829	0.21212	0.23031	0.24706	0.24683
	2.12072	1.96361	0.54431	0.25810	0.22148	0.18410	0.17962	0.18814	0.21156	0.21623	0.23138
1.5	0.13815	0.15945	0.29881	0.35199	0.36035	0.31712	0.33244	0.31035	0.30316	0.32061	0.31060
	3.07854	2.32459	1.70401	0.86157	0.45843	0.35382	0.35891	0.30941	0.30274	0.31870	0.29598
	0.17697	0.15577	0.37208	0.55335	0.55512	0.51438	0.51368	0.48383	0.49249	0.42680	0.47090
	3.89041	3.15115	2.58508	1.76622	0.99471	0.65380	0.58423	0.53832	0.50869	0.43904	0.47885
	0.17079	0.14980	0.44026	0.67499	0.86090	0.84880	0.85450	0.69410	0.67099	0.66948	0.68146
	4.23216	3.34039	3.09945	2.79798	1.99287	1.32447	1.07203	0.79730	0.75204	0.69418	0.69721

Table 12: Mean square error of  $\hat{\kappa}_M$  (top raw) and  $\hat{\kappa}_L$  (bottom raw) for GvMF<sub>3,3</sub> distribution, for different values of  $\alpha$  (rows) and  $\kappa$  (columns)

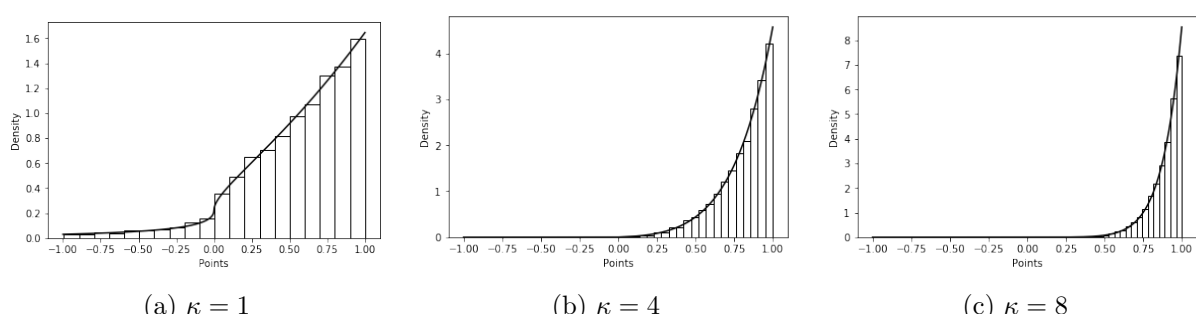


Figure 6: Density  $f_1$  from (56) for  $\alpha = 0.5$  and different values of  $\kappa$ .

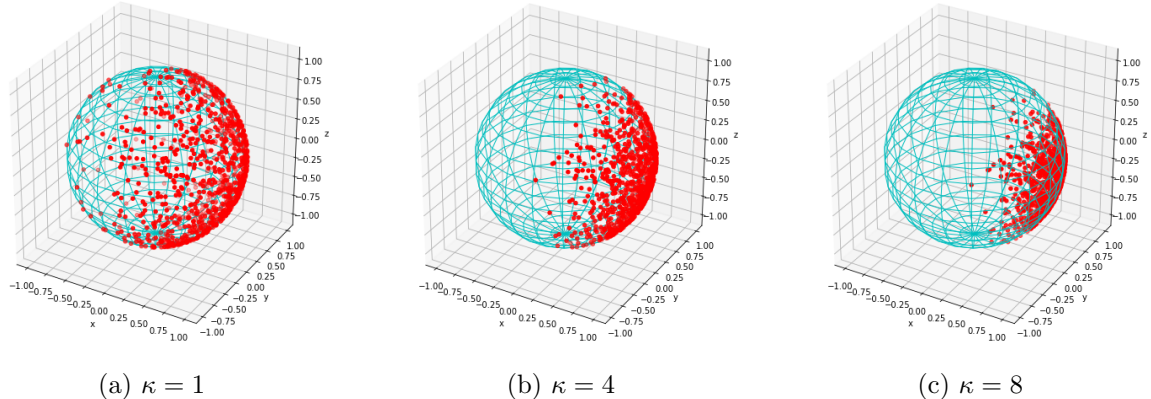


Figure 7: Realisations of  $X \sim \text{GvMF}_{1,3}(\kappa, \alpha, \mu)$  with  $\alpha = 0.5$  and different values of  $\kappa$ .

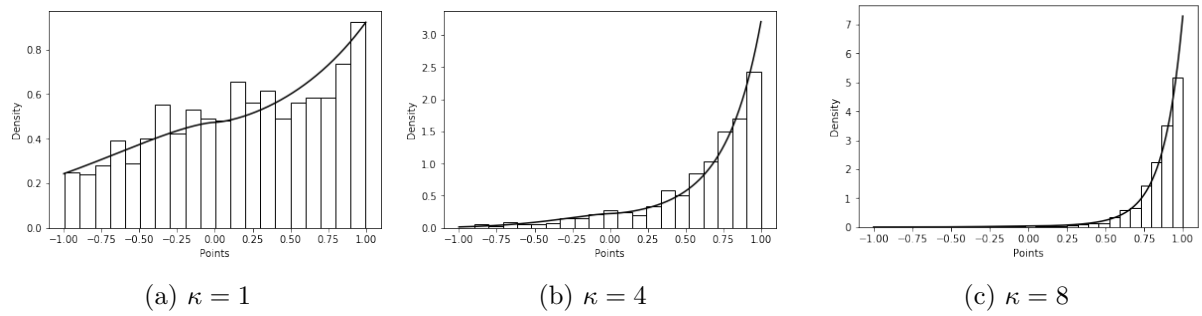


Figure 8: Density  $f_1$  from (56) for  $\alpha = 1.5$  and different values of  $\kappa$ .

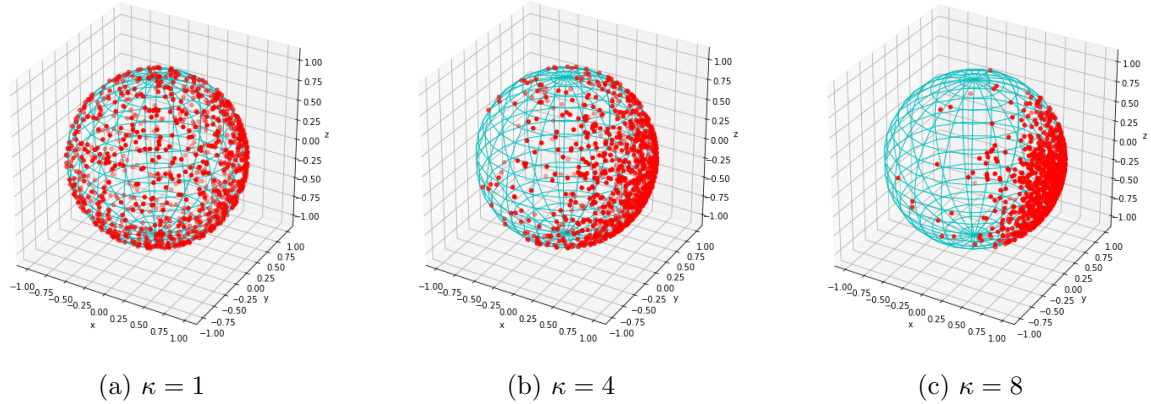


Figure 9: Realisations of  $X \sim \text{GvMF}_{1,3}(\kappa, \alpha, \mu)$  with  $\alpha = 1.5$  and different values of  $\kappa$ .

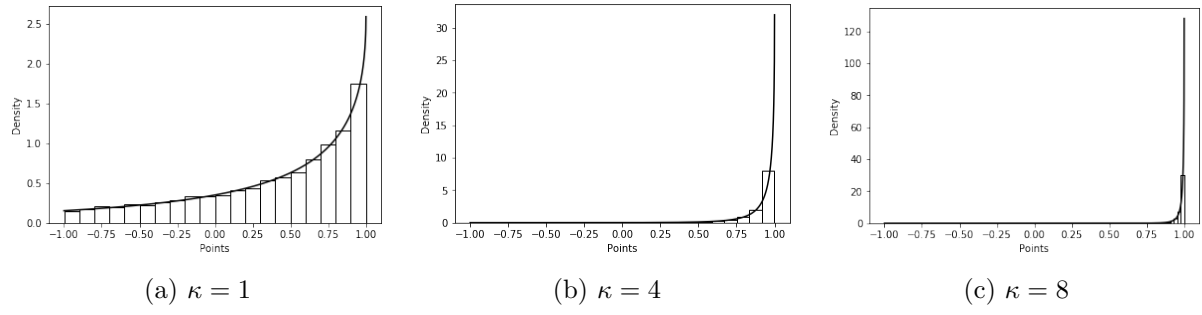


Figure 10: Density  $f_2$  from (57) for  $\alpha = 0.5$  and different values of  $\kappa$ .

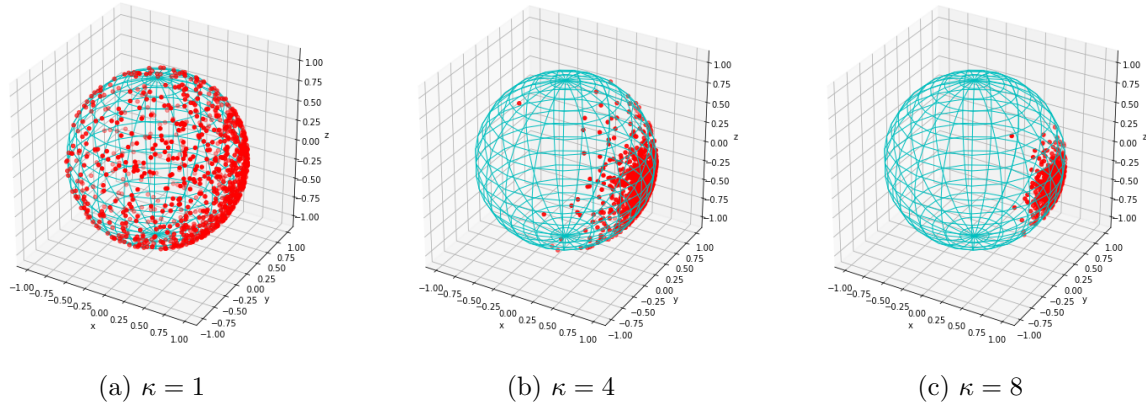


Figure 11: Realisations of  $X \sim \text{GvMF}_{2,3}(\kappa, \alpha, \mu)$  with  $\alpha = 0.5$  and different values of  $\kappa$ .

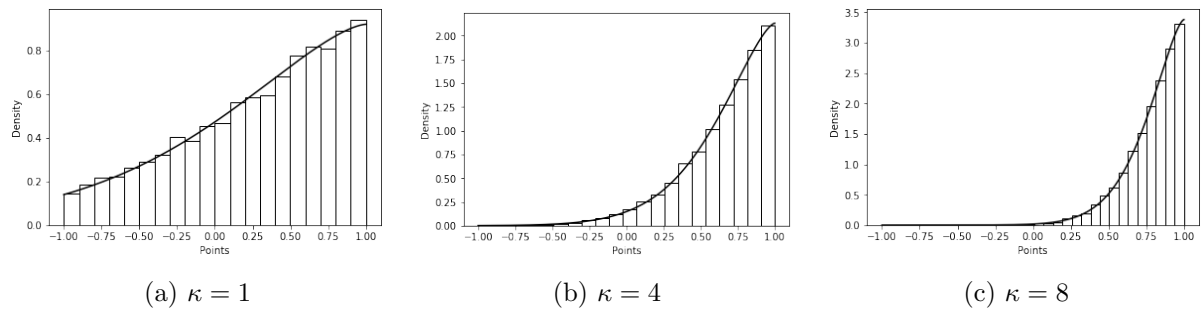


Figure 12: Density  $f_2$  from (57) for  $\alpha = 1.5$  and different values of  $\kappa$ .

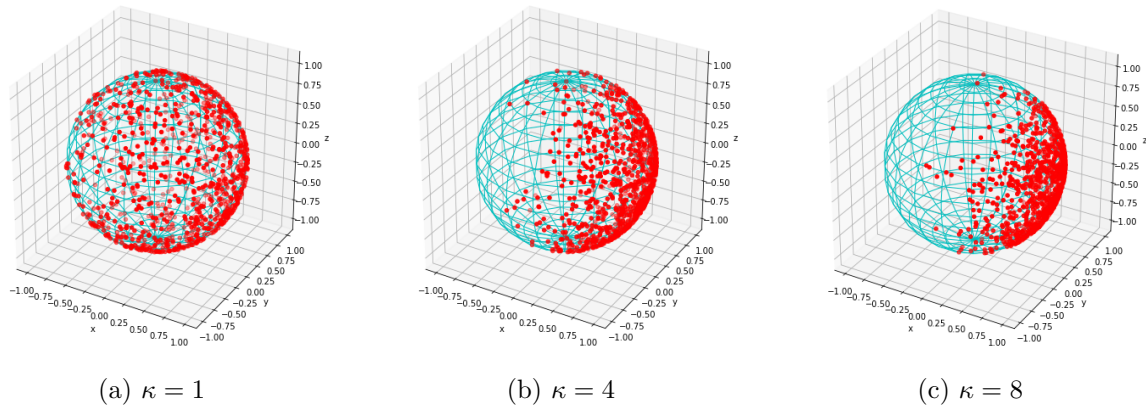


Figure 13: Realisations of  $X \sim \text{GvMF}_{2,3}(\kappa, \alpha, \mu)$  with  $\alpha = 1.5$  and different values of  $\kappa$ .

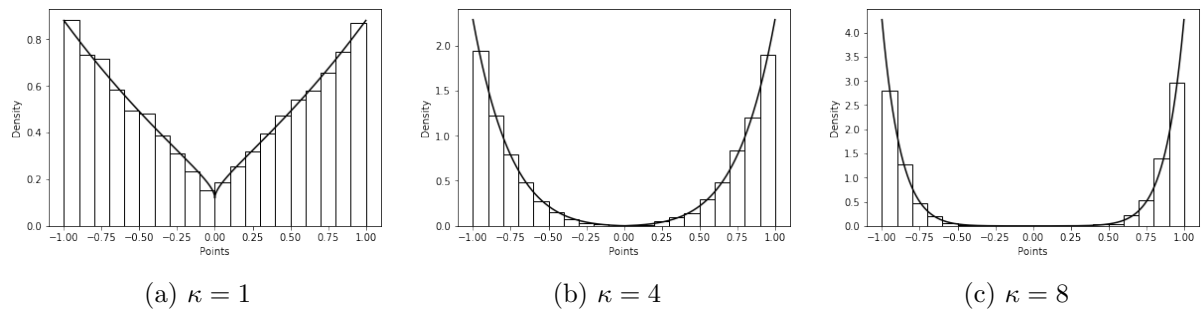


Figure 14: Density  $f_3$  from (58) for  $\alpha = 0.5$  and different values of  $\kappa$ .

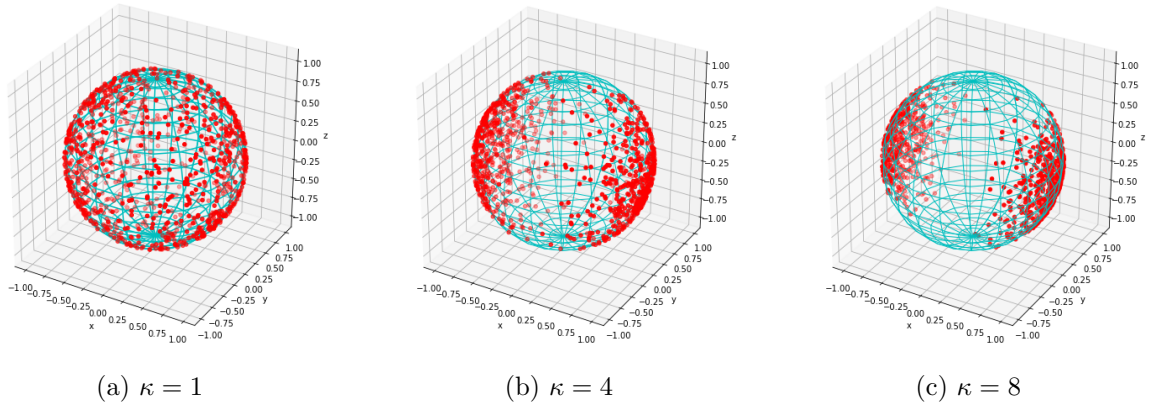


Figure 15: Realisations of  $X \sim \text{GvMF}_{3,3}(\kappa, \alpha, \mu)$  with  $\alpha = 0.5$  and different values of  $\kappa$ .

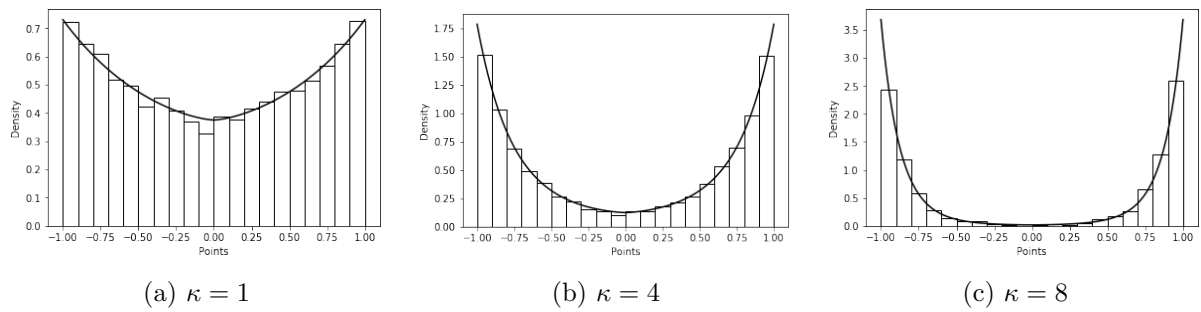


Figure 16: Density  $f_3$  from (58) for  $\alpha = 1.5$  and different values of  $\kappa$ .

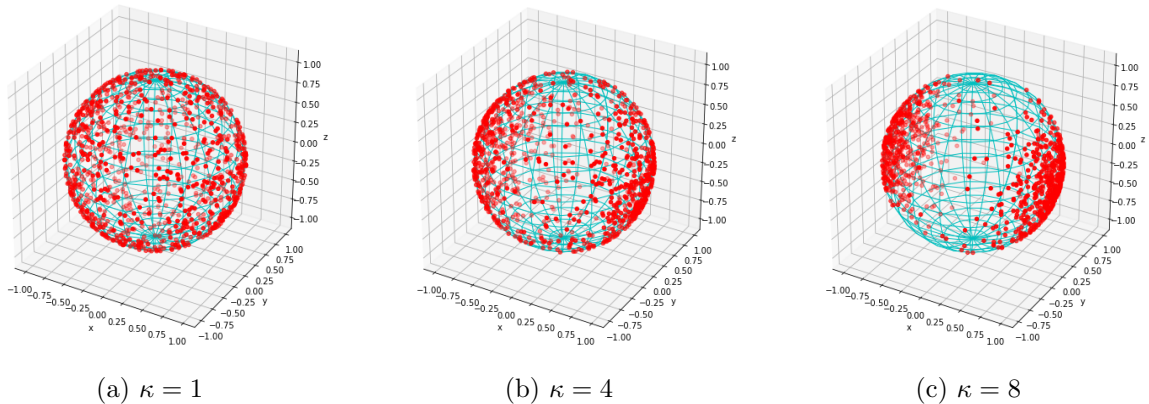


Figure 17: Realisations of  $X \sim \text{GvMF}_{3,3}(\kappa, \alpha, \mu)$  with  $\alpha = 1.5$  and different values of  $\kappa$ .